

Topology and RSSI-based Localization for Ad Hoc Networks

(M.Sc. Thesis)

Sofia Nikitaki

Paris

June 2009

**DEPARTMENT OF COMPUTER SCIENCE
LRI (PROJECT HIPERCOM), UNIVERSITY OF PARIS SOUTH 11
AND UNIVERSITY OF CRETE**

Topology and RSSI-based Localization for Ad Hoc Networks

Submitted in the 29th of June 2009 to the committee below
In partial fulfilment of the requirements for the degree of
Master in Computer Science
Under the common French-Greek graduate programme

Author:

Sofia NIKITAKI

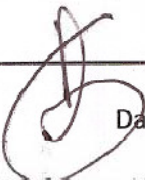
Supervisor :



Khaldoun AL AGHA

Professor, University Paris South 11

Member :



Daniel ETIEMBLE

Professor, University Paris South 11

Grade : 16/20

Comments :

Excellent work.

Université Paris Sud 11 - Orsay
Master Recherche Informatique
Bâtiment 490
91405 Orsay CEDEX

To my family...

Topology and RSSI-based Localization for Ad Hoc Networks

Sofia Nikitaki

M.SC. Thesis

**Department of Computer Science
LRI (Project HIPERCOM), University of Paris South XI
and University of Crete**

Abstract

In wireless ad hoc networks, node's location information is useful for efficient routing and location-aware applications. Ad hoc localization systems permit nodes in sensor networks to fix their positions in a global coordinate system. This is usually performed with the use of location measurement devices, such as GPS. However, low-end systems or indoor systems, which cannot use GPS, must locate themselves based only on information available locally, such as distance of neighboring nodes. In this thesis, we propose the development of a 'cooperative' geolocalization protocol based on the properties of an ad hoc network. Particularly, we introduce a localization framework that is compatible with a fully distributed and constantly evolving environment and it considers a priori and reliability information. It is an improvement of the Kamada-Kawai method, a popular localization method first used in graph theory. The weakness of Kamada-Kawai method is that it does not mention all the available information. The proposed localization algorithm observes the whole network topology and precisely indicates that if the unlocated node is not an one-hop neighbour with another node it is likely that their distance is maximal. Each unknown node is aware of the network topology. The distances between neighboring nodes are calculating by using the RSSI technique. Moreover, real RSSI measurements have been performed in order to find the correlation between the signal strength and the distance. The performance of our approach is evaluated with simulations in real-world conditions in different environments.

Contents

| | |
|---|----|
| 1. Introduction..... | 1 |
| 2. Background Theory and Related work | 3 |
| 2.1 Localization sensing techniques..... | 3 |
| 2.1.1 Triangulation..... | 4 |
| 2.1.2 Scene analysis | 7 |
| 2.1.3 Proximity..... | 7 |
| 2.2 Existing localization systems | 8 |
| 2.3 Localization algorithms for wireless ad hoc networks..... | 13 |
| 2.3.1 Existing distance measurements technologies..... | 13 |
| 2.3.2 Radio communication constraint models..... | 14 |
| 2.3.3 Radio communication | 14 |
| 2.3.4 Propagation methods..... | 14 |
| 2.3.5 Position estimation..... | 15 |
| 2.3.6 Refinement..... | 17 |
| 2.3.7 Impact of anchor density..... | 17 |
| 2.3.8 Localization Accuracy Metrics | 18 |
| 2.3.9 Reported precision | 18 |
| 3. Methodology - Position Estimation | 21 |
| 3.1 T.Kamada and S.Kawai method..... | 21 |
| 3.2 Weighted Min Max method | 24 |
| 3.3 Min Max method..... | 27 |
| 3.4 RSSI model | 30 |
| 4. Evaluation | 33 |
| 4.1 Performance analysis..... | 33 |
| 4.2 Network Generator- Simulations | 38 |

| | |
|---|----|
| 5. Received Signal Strength Indicator | 47 |
| 5.1 Measurements..... | 47 |
| 5.1.1 Outdoor environment..... | 47 |
| 5.1.2 Indoor environment..... | 51 |
| 5.2 RF Propagation loss model | 54 |
| 5.2.1 Outdoor environment..... | 54 |
| 5.2.3 Indoor environment..... | 55 |
| 6. Conclusion | 59 |
| 7. References..... | 61 |

List of Figures

| | |
|---|----|
| Figure 2.1: Determining 2D position using lateration requires distance measurements between the object 'X' and 3 non-collinear points [6]..... | 4 |
| Figure 2.2: Location-sensing based on Time of Arrival (TOA)..... | 5 |
| Figure 2.3: Location-sensing based on Time Difference of Arrival (TDOA)..... | 5 |
| Figure 2.4: Location-sensing based on Angle of Arrival (AOA)..... | 7 |
| Figure 2.5: Monitoring wireless cellular access point..... | 8 |
| Figure 2.6: The GPS constellation consists of six orbital planes with four satellites in each plane. Each satellite is identified with a two-character code: a letter identifies the orbital plane (A through F) and a number identifies the satellite number in plane (1 through 4) [8]...9 | 9 |
| Figure 2.7: This picture shows four generations of the Active Badge. Bottom left, the first version, with a unique five bit code. Bottom right, the second version, with a ten bit code. Top left the third, current, version, with a forty-eight bit code, bi-directional capabilities, and an on-board 87C751 microprocessor..... | 10 |
| Figure 2.8: Radio communication constraints. (a) Radio constraint, (b) Angular constraint, (c) N-hop neighborhood constraint..... | 14 |
| Figure 2.9: (a) DV-Hop propagation method, (b) Euclidean propagation method..... | 15 |
| Figure 2.10: Bounding-box examples. (a) Distance-based approach, (b) Radio pattern-based approach..... | 16 |
| Figure 3.1: Kamada-Kawai method..... | 25 |
| Figure 3.2: Weighted Min Max method..... | 25 |
| Figure 4.1: Kamada Kawai method in a network of 3 nodes..... | 34 |
| Figure 4.2: Weighted Min Max method in a network of 3 nodes..... | 34 |
| Figure 4.3: Weighted Min Max method in a network of 4 and 5 nodes, respectively..... | 35 |
| Figure 4.4: Network topology..... | 36 |
| Figure 4.5: Kamada Kawai method in a network of 10 nodes. Node 1 implements the localization algorithm..... | 36 |
| Figure 4.6: Weighted Min Max method in a network of 10 nodes. Node 1 implements the localization algorithm..... | 37 |
| Figure 4.7: Min Max method in a network of 10 nodes. Node 1 implements the localization algorithm..... | 38 |
| Figure 4.8: Schema of simulation..... | 39 |

| | |
|--|----|
| Figure 4.9: Network topology..... | 40 |
| Figure 4.10: Weighted Max Method. The final location error is 19.1613 (m)..... | 41 |
| Figure 4.11: Weighted Max Method. The final location error is 49.9477 (m)..... | 42 |
| Figure 4.12: Location error of the sensors in the network at figure 4.9. The error depends on the Location algorithm each node runs..... | 43 |
| Figure 4.13: (a) Weighted Min Max location error (m). (b) Error of the Euclidian distance due to RSSI measurements for different values of path loss exponent..... | 43 |
| Figure 4.14: Location error of the sensors in the network at fig. 4.9. The error depends on the Location algorithm each node runs..... | 44 |
| Figure 4.15: (a) Weighted Min Max location error (m). (b) Error of the Euclidian distance due to RSSI measurements for different values of path loss exponent..... | 45 |
| Figure 5.1: Testbed area ‘Parc Montsouris’. The experiments took place at the red square... | 48 |
| Figure 5.2: RSSI measurements from the outdoor experiment in ‘Parc Montsouris’ | 49 |
| Figure 5.3: RSSI variability | 50 |
| Figure 5.4: RSSI compartment at an outdoor environment..... | 50 |
| Figure 5.5: Floor plan of the testbed area ICS-FORTH. The experiments took place at the green square | 52 |
| Figure 5.6: 60 RSSI measurements collected every one meter during the experiment in ICS-FORTH. | 53 |
| Figure 5.7: RSSI compartment at an indoor environment..... | 53 |
| Figure 5.8: Outdoor propagation model for RSSI measurements..... | 55 |
| Figure 5.9: Indoor propagation model for RSSI measurements. | 56 |

List of tables

| | |
|---|----|
| Table 2.1: Location system properties [16] | 13 |
| Table 2.2: Reported precision for the positioning algorithms in Ad hoc networks | 19 |
| Table 4.1: Data of the Ad hoc network that consists of 10 nodes. | 40 |
| Table 4.2: Data of the Ad hoc network that consists of 10 nodes. | 44 |
| Table 4.3: Localization performance of the Weighted Min Max method in 4 different environments..... | 45 |
| Table 5.1: Characteristics of the nodes used in the outdoor experiment | 48 |
| Table 5.2: Characteristics of the nodes used in the indoor experiment. | 51 |

CHAPTER 1

1. Introduction

Recent advances in the technologies of mobile devices and wireless communication have given rise to an increasingly popular form of networking, called mobile ad hoc networking. A mobile ad hoc network (MANET) consists of small, versatile and powerful mobile computing devices (nodes). It is typically formed at short notice and does not make use of any fixed networking infrastructure. Since, these networks provide an interface to the physical world, it is necessary for each sensor node to learn its location in the physical space.

As a result, localization-based services have gained considerable attention from the academia and industry. For sensors networks the ability of nodes to determine their position through automatic means is recognized as an essential capability. Many applications with sensor networks demand localization information, such as habitat monitoring, health caring, battle-field surveillance, enemy tracking and environment observation.

To obtain the location information, the Global Positioning System (GPS) [8] could be used. However, this approach is inappropriate for large scale ad hoc networks due to several reasons. The cost parameter and the constraints of power consumption are very important. Moreover inaccessibility does not make GPS the most attractive solution since nodes may be deployed indoors or GPS reception might be obstructed by climatic conditions.

In ad hoc localization, distributed algorithms enable nodes to automatically determine their *relative* positions, after deployment, in a common coordinate system. If it is necessary, a number of *anchor* nodes that already know their position (through some external means, i.e. GPS) are used in the same coordinate system.

There are several requirements a positioning algorithm has to satisfy. Firstly, there is the need for a distributed system. In a large ad hoc network with a big amount of nodes it is obvious that a hop by hop manner could put too high a strain on the nodes close to the base station/server. Moreover, the algorithm must have low signalling complexity. Finally, the algorithm has to be insensitive to anchor placement and the number of the anchor nodes needed for a good localization should be minimum.

The performance of ad hoc localization depends upon several factors: the accuracy of ranging, the density of node placement, the relative density of anchors, as well as the particular position fixing schemes in use.

In this work we formulate the localization problem as a constrained least square problem. Particularly, our approach finds the coordinates of the unlocated node that maximize the sum from the unknown distances under the constraint that all known distances are respected. We especially underline techniques like (Received Signal Strength Indicator) RSSI whose complexity and cost is low enough to realize a simple implementation. We are going to deal with the ‘cooperative localization’, when each node or sensor decides its position due to some shared information with his neighbors.

The present thesis is organized as follows. Chapter 2 presents the most important localization techniques and the state of the art on the geolocalization. In Chapter 3, we describe the formulation of the problem and the positioning algorithm that we use. In Chapter 4, the performance analysis of our system is demonstrated via simulations. Finally, in Chapter 5, we present the experiments we performed in order to collect the signal strengths measurements in outdoor and indoor environment.

CHAPTER 2

2. Background Theory and Related work

Location sensing systems can be classified according to their dependency and use of an infrastructure, specialized hardware, signal modalities, training, methodology and models for estimating distances and position, coordination system (absolute or relative), location description (physical or symbolic), scale, device identification, classification, recognition, cost, privacy, accuracy and precision requirements [16]. The distance can be estimated using *signal strength*, *time of arrival* or *angle of arrival* measurements, if a signal attenuation model, the velocity and the angle of a signal, respectively, are known. A result is considered *accurate*, if it is consistent with the true or accepted value for the result. Unlike accuracy, *precision* refers to the repeatability of measurements.

Several localization systems devices of different modality, such as radio (RADAR [9]), infrared (Active Badge [12]), ultrasonic (Cricket [10], Active Bat [15]) while others physical contact with pressure (Smart Floor [14]), exists to infer the position.

Ad hoc localization systems permit nodes in a sensor network to fix their positions in a global coordinate system using a relatively small number of *anchor nodes* that know their position through external means. Location information provides context to sensed data therefore such systems have gained considerable attention from the academia.

2.1 Localization sensing techniques

There are three common techniques in location sensing: triangulation, scene analysis and proximity [6].

2.1.1 Triangulation

The triangulation location sensing technique uses the geometric properties of the triangles to compute object locations.

Lateralation

Lateralation, one of the subcategories of triangulation, computes the position of an object by measuring its distance from multiple reference positions. Particularly, in order to calculate an object's position in two dimensions requires distance measurements from 3 non-collinear points as shown in Figure 2.1

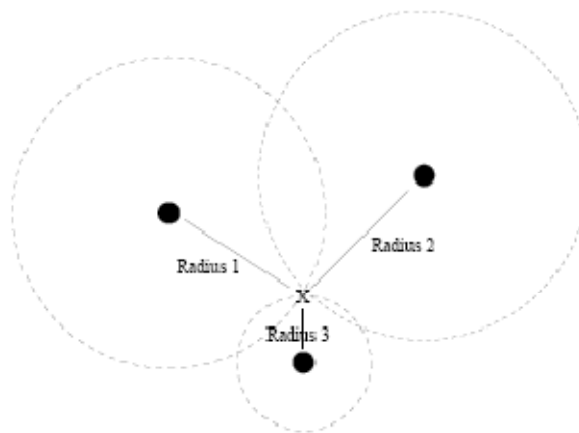


Figure 2.1: Determining 2D position using lateralation requires distance measurements between the object 'X' and 3 non-collinear points [6]

The distance between the base station and the mobile station can be estimated by measuring the time-of-flight which is the time it takes the signal to travel between them or the amount of signal attenuation along the way.

The most common methods based on the approach of time-of-flight are Time of Arrival (TOA), Time Difference of Arrival (TDOA) and Enhanced Observed Time Difference (E-OTD).

The TOA method works by measuring the arrival time of a known signal sent from a (mobile) node received at three or more measurements units. Synchronization of the measurement units is essential. Therefore, this method requires additional measurement unit hardware in the network at the geographical vicinity of the (mobile) node, so as to accurately measure the TOA of the signal bursts.

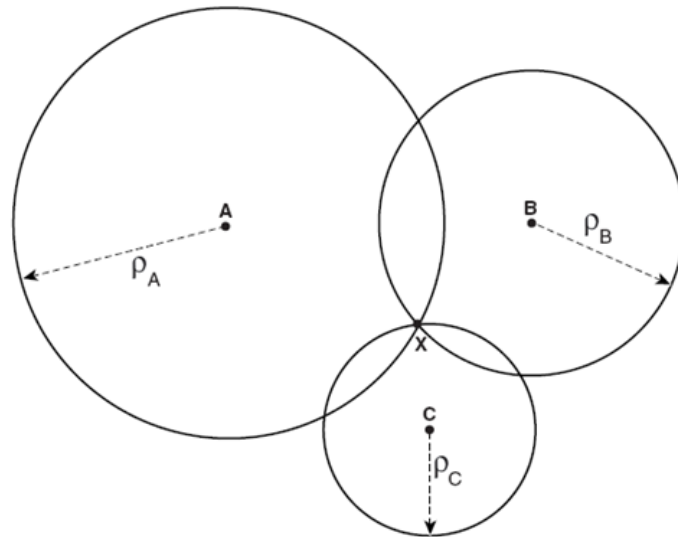


Figure 2.2: Location-sensing based on Time of Arrival (TOA).

TDOA uses the range differences between receivers. When a transmitter sends two types of signals simultaneously, the receiver can detect the difference in the time of arrival between the two types of signals. These range differences can be described as a hyperbolic curve in 2D or a hyperboloid in 3D space and can be used to compute the distance between the communication pairs.

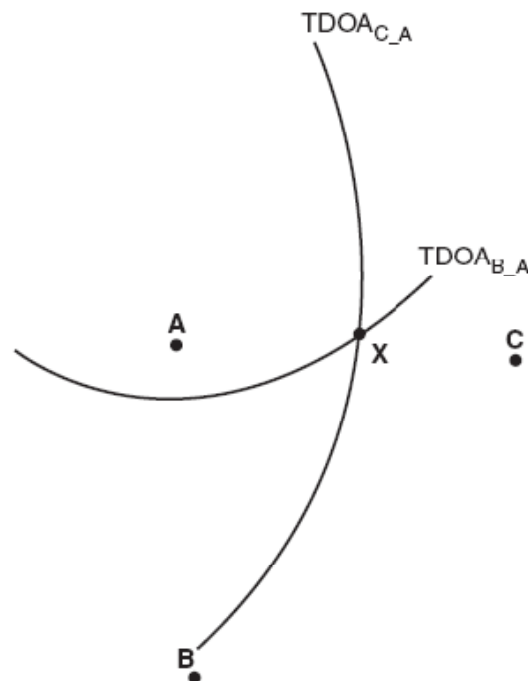


Figure 2.3: Location-sensing based on Time Difference of Arrival (TDOA)

In E-OTD method the mobile node performs the time measurement of beacon signals nearby base stations. This method does not require synchronization with the network.

Furthermore, the intensity of emitted signal strength decreases as the distance from the emission source increases. As a result, the distance can be estimated based on a propagation model, which predicts the average signal strength at a given distance from the transmitter. The free-space propagation model assumes the ideal propagation condition that there is only one clear line-of-signal path between transmitter and receiver. The following equation calculates the received signal power in free space at distance d from the transmitter.

$$P_r(d) = \frac{P_t G_t G_r \lambda^2}{(4\pi)^2 d^2 L} \quad (1.1)$$

where P_t is the transmitted signal power, G_t and G_r are the antenna gains of the transmitter and the receiver respectively. $L(L \geq 1)$ is the system loss and λ is the wavelength. The formula (1) leads to a path loss factor for free-space propagation of $1/R^2$ for the decrease in received power with distance. When a ground reflection is present, the path loss can be as much as $1/R^4$ in the worst case. In practice, the resulting path loss can be expressed as $1/R^n$ where n may vary from 2 to 6 [2].

Angulation

The angulation method uses the angles to determine the position of an object. In the Angle of Arrival (AOA) technique the mobile node uses the angles from two or more base stations in order to find its position by the intersection of the arrival directions. Therefore, the AOA method requires special antenna arrays at mobile node. The AOA method is susceptible to multipath interference, caused by the reflection of the true signal from surrounding objects. Since this technology uses line-of-sight (LOS) signal, if there is no LOS it will take a reflected signal that may not be coming from the direction of the mobile object. Therefore, the accuracy of the AOA method reduces as the distance between the mobile object and the base station increases due to fundamental limitations of the devices used to measure the arrival angles.

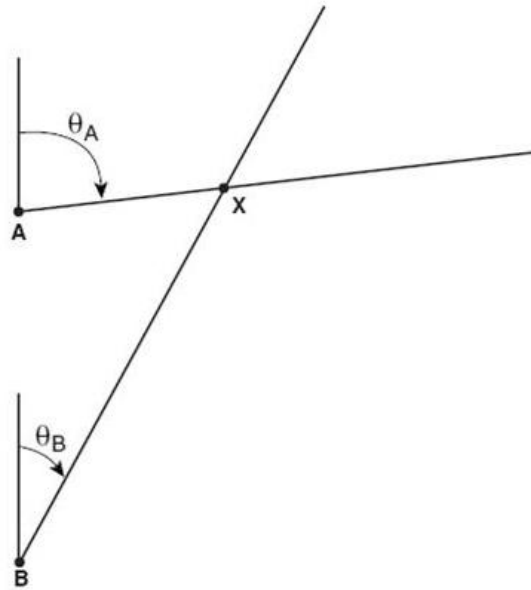


Figure 2.4: Location-sensing based on Angle of Arrival (AOA)

2.1.2 Scene analysis

The scene analysis location sensing technique uses features of a scene observed from a particular vantage point to draw conclusions about the location of the observer or objects in the scene. All the methods that use scene location sensing consist of two phases, the offline training phase and the online estimation phase. In the offline phase, the location determination system creates a radio map, which is a database of various locations and their corresponding signal strength fingerprints. In the online phase, location is determined by querying this radio map with the fingerprint extracted at that particular location. The advantage of scene analysis is that the location of the objects can be inferred using passive observation and features that do not correspond to geometric angles or distances. Another advantage is that they can provide accurate position estimation in cluster environments with multipath and NLOS propagation. However, the main disadvantage is that the radio map should be large enough and representative of the current environment for accurate position estimation. As a result, the database must be updated frequently enough so that the channel characteristics in the offline and online phases do not differ significantly. Such an update requirement is extremely time consuming.

2.1.3 Proximity

A proximity location sensing technique defines when an object is “near” a known location. There are three general approaches to sensing proximity:

Detecting physical contact. Technologies for sensing physical contact include pressure sensors, touch sensors and capacitive field detectors [4].

Monitoring wireless cellular access points. The following figure illustrates an example of monitoring when a mobile device is in range of one or more access points in a cellular network. The cell geometry is used in the implementation. Objects 'X', 'Y', and 'Z' are located by monitoring their connectivity to one or more access point in a wireless cellular network.

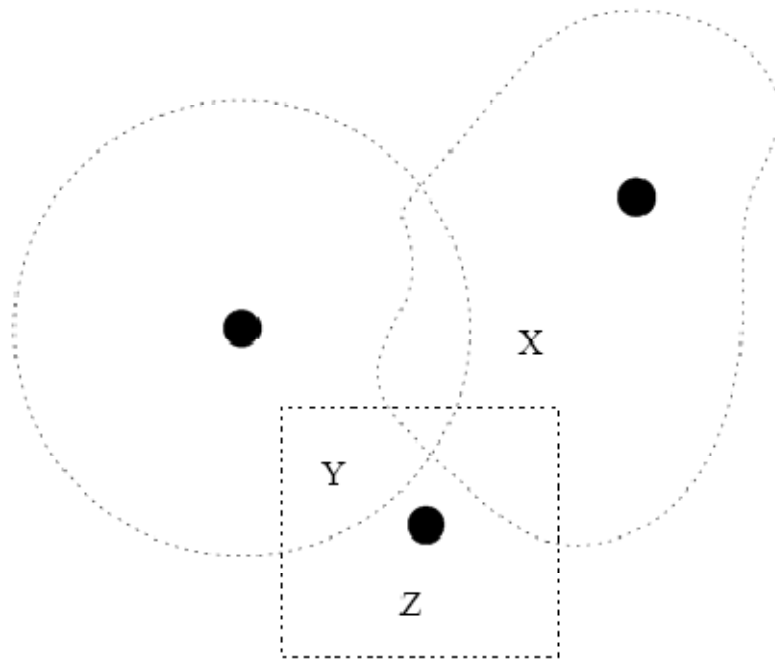


Figure 2.5: Monitoring wireless cellular access point

Observing automatic ID systems. Observing automatic identification systems is an implementation which uses systems such as credit card point-of-sale terminals, computer login histories, land-line telephone records, electronic card lock logs, and identification tags such as electronic highway E-Toll systems, UPC product codes, RFID badges. Assuming that the location of the device is known the location of the mobile object can be deduced.

2.2 Existing localization systems

Location systems have been successfully built using a variety of technologies. In this section the most popular and widely used systems are presented.

GPS

GPS consists of three components: satellites, control stations and GPS receivers [8]. A GPS receiver calculates its position by precisely timing the signals sent by the GPS satellites high above the Earth. The receiver measures the transit time of each message and computes the distance to each satellite. The GPS system consists of 24 orbiting operational satellites which can transmit very low power radio signals, allowing any GPS receiver to determine its position on Earth (Figure 2.6). GPS control system monitors the satellites, providing them with correct orbital and clock data.

The receiver, in order to determine the position, needs to know the location of at least four satellites and the distance between them. The approximate location of the satellites is obtained directly from the satellites themselves. This approximation can be adjusted by using data from control stations.

The distance from the receiver to the satellite is calculated as the product of radio speed and the radio travel time between them. The travel time is estimated from the difference of the ‘pseudo-random’ code generated by the satellite and the receiver at the same time. With the information of four or more satellites, the position of the receiver can then be determined.

An extension of GPS system is the Differential GPS (DGPS). DGPS uses stations to broadcast position correction beacons. With these correction messages, GPS receivers can provide real-time difference corrections on the received satellite signals.

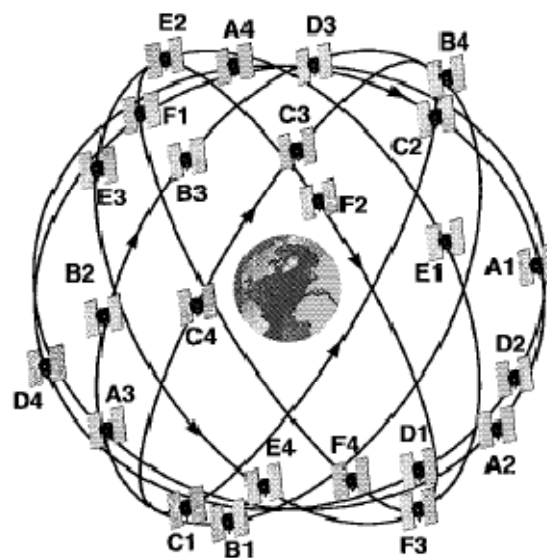


Figure 2.6: The GPS constellation consists of six orbital planes with four satellites in each plane. Each satellite is identified with a two-character code: a letter identifies the orbital plane (A through F) and a number identifies the satellite number in plane (1 through 4) [8]

RADAR

RADAR is an RF-based system for locating and tracking users inside buildings [9]. RADAR employs signal strength maps that integrate signal strength measurements acquired during the training phase from APs at different positions with the physical coordinates of each position. Each measured signal strength vector is compared against the reference map and the coordinates of the best match will be reported as the estimated position. 90% of the time the hosts can be located with at most six meters of error with a sampling density of one sample every 13.9m² and 19.1m² of their testbed using the signal from three and five APs, respectively.

Active Badge

The Active Badge consists of a cellular proximity system that uses diffuse infrared technology [12]. Each person the system can locate wears a small infrared badge (Figure 2.7). The badge emits a globally unique identifier every 10 seconds or on demand. A central server collects this data from fixed infrared sensors around the building, aggregates it, and provides an application programming interface for using data. The Active Badge system provides absolute location information. The system suffers in the case of fluorescent lightning and direct sunlight, because of the spurious infrared emissions these light sources generate.

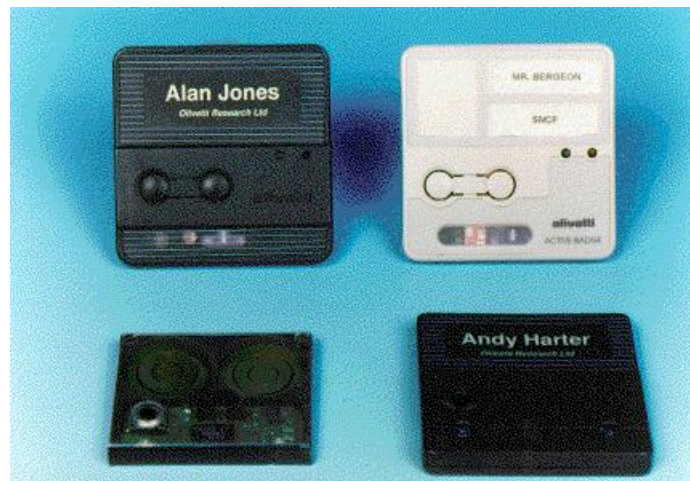


Figure 2.7: This picture shows four generations of the Active Badge. Bottom left, the first version, with a unique five bit code. Bottom right, the second version, with a ten bit code. Top left the third, current, version, with a forty-eight bit code, bi-directional capabilities, and an on-board 87C751 microprocessor.

Active Bat

The Active Bat location system uses an ultrasound time-of-flight lateration technique to provide more accurate physical positioning than Active Badges [15]. The system consists of a controller that sends a radio signal and a synchronized reset signal simultaneously to the ceiling sensors using a wired serial network. Bats respond to the radio request with an ultrasonic beacon. Ceiling sensors measure time-of-flight from reset to ultrasonic pulse. Active Bat applies statistical pruning to eliminate erroneous sensor measurements caused by a sensor hearing a reflected pulse instead of one that travelled along the direct path from the Bat to the sensor. A relatively dense deployment of ultrasound sensors in the ceiling can provide within 9 cm of true position 95% of the measurements. However, Active Bats requires large infrastructure and maintenance cost.

E911

E911 is a location service which is used in order to locate any phone that makes a 911 emergency call in United-States [13]. The system incorporates the use of the GPS in certain mobiles, triangulation with the basic stations and a combination of these technologies. The caller's location is determined by the geographic location of the cellular phone within 100 meter accuracy. E911 had a considerable impact on localization services because it justified the development of many systems of localization for the cellular networks but also for the WLAN.

Smart Floor

Smart Floor is a system for biometric user identification based on footsteps profile [14].The system employs a pressure sensor grid installed in all floors to determine presence information. It relies on uniqueness of footstep profiles within a small group of people to provide recognition accuracy. Specifically, the recognition rate is 93%. Moreover, Smart Floor can accurately determine positions in a building without requiring from users to wear tags or carry devices. However, the system has the disadvantages of poor scalability and high incremental cost because the floor of each building in which Smart Floor is deployed must be physically altered to install the pressure sensor grid.

Cricket

Cricket [10],[11] is an indoor localization method developed in MIT in 2000 which uses a combination of RF and ultrasound. It allows applications running on mobile and static nodes to learn their physical location by using *listeners* that hear and analyze information from *beacons* spread throughout the building. Cricket does not rely on centralized management taking into consideration user privacy. Particularly, a beacon sends an RF message and an ultrasonic pulse concurrently. When the listener hears the RF signal, it uses the first few bits as training information and then turns on its ultrasonic receiver. It then listens for the ultrasonic pulse, which usually arrives a short time later. As a result, it determines the distance to the beacon from the time difference between the receipt of the first bit RF information and the ultrasonic distance.

VOR

The VHF Omnidirectional Range navigation system, VOR, is an aircraft navigation system [18]. The VOR facility transmits two signals at the same time. One signal is constant in all directions, while the other is rotated about the station. The airborne equipment receives both signals, looks at the difference between the two signals, and interprets the result as a *radial* from the station. So, the road of the plane is estimated via AOA.

Synthesis

Researchers in academia and industry have created numerous location-sensing systems that differ with respect to accuracy, coverage, frequency of location updates, cost of installation and maintenance. Table 2.1 exposes a synthesis of the location systems mentioned above. In Table 2.1 the checkmarks indicate that localized location computation (LLC) or recognition applies to the system. Moreover, for each technology the accuracy, precision and scale are reported.

| Technology Name | Properties | | | Classification Criteria | |
|-----------------|--|-----|-------------|-------------------------|--|
| | Technique | LLC | Recognition | Accuracy & Precision | Scale |
| GPS | Radio time-of-flight lateration | ✓ | | 1-5 meters (95-99%) | 24 satellites worldwide |
| RADAR | 802.11 RF scene analysis % triangulation | | ✓ | 3-4.3 meters (50%) | |
| Active Badges | Diffuse infrared cellular proximity | | ✓ | Room size | 1 base per room, badge per base per 10 sec |

| | | | | | |
|------------------------------------|--------------------------------------|---|---|-------------------------------------|--|
| Active Bats | Ultrasound time-of-flight lateration | | ✓ | 9 cm (95%) | 1 base per 10m ² , 25 computations per room per sec |
| Cricket | Proximity, lateration | ✓ | | 4x4 ft. regions ($\approx 100\%$) | ≈ 1 beacon per 16 sq. ft. |
| Smart Floor | Physical contact proximity | | ✓ | Spacing of pressure sensors (100%) | Complete sensor grid per floor |
| VHF Omni directional Ranging (VOR) | Angulation | ✓ | | 1° radial ($\approx 100\%$) | Several transmitters per metropolitan area |

Table 2.1: Location system properties [16]

2.3 Localization algorithms for wireless ad hoc networks

Node localization has been the topic of active research and many systems have made their appearance in the past few years. In this section a summary of localisation algorithms for wireless ad hoc networks is presented.

In the general model of wireless ad hoc sensor networks there are usually some landmarks or nodes named *anchor* nodes whose position information is known within the area to facilitate locating all sensors in a sensor network. All the other nodes are called normal nodes.

Generally the location algorithms contain three steps:

1. Through broadcast, each node measures the pair-wise distance (or angle) from each other; furthermore, each node can estimate their distance from anchor nodes.
2. Each normal node derives a position based on the anchors' position information.
3. Each node iteratively refines the position estimation with the constraints of neighbours' information.

2.3.1 Existing distance measurements technologies

Based on the applied hardware and the operating environment, distance measurement technologies can be categorized into two main categories. The first category is satellite positioning technologies and includes Global Positioning System (GPS), Differential GPS (DGPS), Galileo System (European version of GPS). The second category consists of network based technologies such as TOA, TDOA, AOA with accuracy 100-200 m and the Received Signal Strength Indicator (RSSI).

2.3.2 Radio communication constraint models

Radio communication constraint models are a set of geometric rules that can be used to bind position estimates. They consist of a combination of the radio [20], angular [22] and N-Hop neighbourhood constraint [21],[22].

The radio constraint means that when a node B can hear node A, the distance between them is less than A's radio transmission range. The angular constraint refers to the fact that when a node gets the best reception at a certain angle, then it can estimate the relative angle to the source transmitter which may be a cone. Final, the N- Hop neighbourhood constraint is a combination of individual constraints from neighbours.

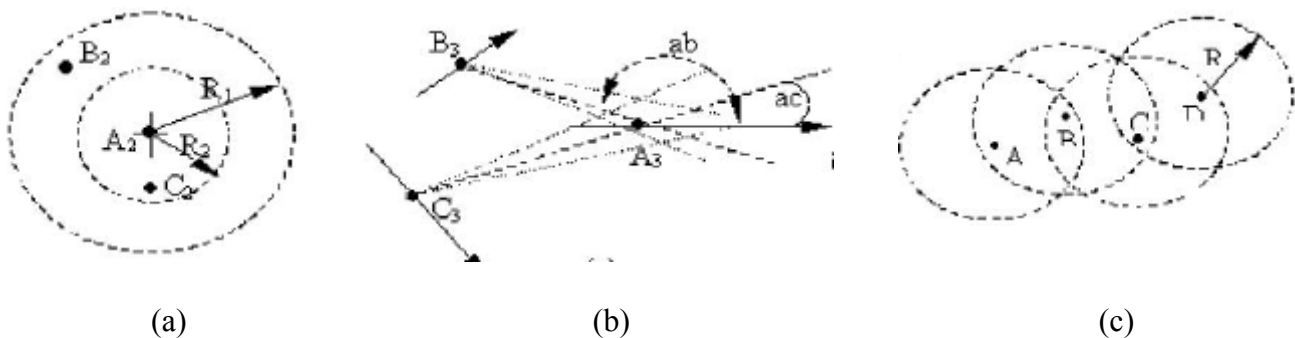


Figure 2.8: Radio communication constraints. (a) Radio constraint, (b) Angular constraint, (c) N-hop neighborhood constraint

2.3.3 Radio communication

In most algorithms the anchor nodes broadcast their position information first. When a node receives an information position it computes his location and rebroadcasts packets to his neighbours. In order to alleviate the expensive flooding one optimization technique is applied. The most common optimization techniques are flood limit [23], hop-count [24] and time stamp method [7]. Flood limit method supposes that when a normal node has recorded enough anchors, it will stop forwarding further information. In the hop-count method, if a node receives multiple packets from the same anchor node, it maintains and rebroadcasts the one with the least hop counts while ignoring all the rest. Finally, in the time stamp method, a Time to Live (*TTL*) stamp is appended to each beacon packet, while outdated packets are dropped silently.

2.3.4 Propagation methods

A normal node in order to estimate its distance from the anchors uses one of the techniques [7]:

1. DV-Hop propagation method

In the DV-Hop method, landmarks propagate their location information inside the network. Each node forwards a distance vector to its neighbours so all nodes in the network get distances, in hops, to the landmarks. When a landmark receives one of the propagated packets with the position of a different landmark, it uses that information to calculate the average hop distance between two landmarks. The computed average hop distance is broadcast back into the network as a correction to previously known hop distances. The corrections are propagated using controlled flooding. Each node will forward a correction from a certain landmark only once in an effort to ensure that nodes will receive only one correction from the closest landmark (Figure 2.9(a))

2. DV-Distance propagation method

The DV-distance approach is similar to DV-hop with the difference that each node measures the pair-wise distance between neighbouring nodes. Similar to the DV-Hop method each node selects and rebroadcasts packets with minimum distance to the anchors.

3. Euclidean propagation method

The Euclidean propagation model uses the true distance measurement to a landmark. In this case, nodes that have at least two distance measurements to nodes that have distance estimates to a landmark can use simple trigonometric relationships to estimate their locations (Figure 2.9(b))

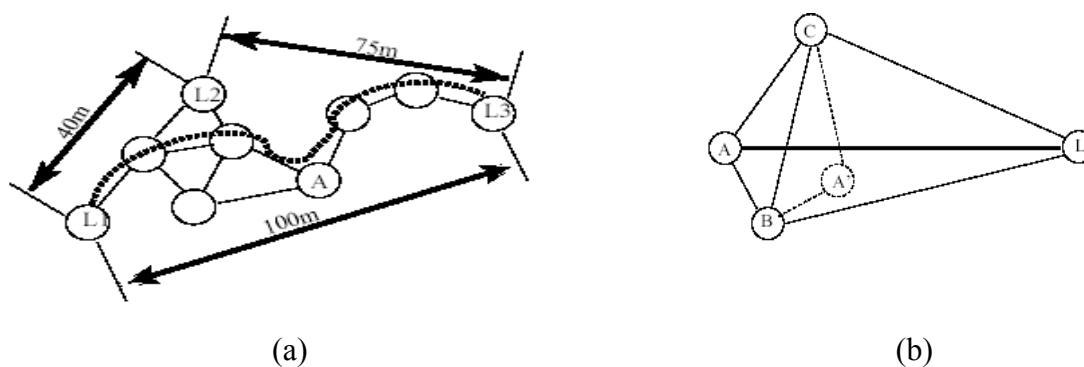


Figure 2.9: (a) DV-Hop propagation method, (b) Euclidean propagation method

2.3.5 Position estimation

In this step of the localisation algorithm every node knows the estimated distance from the anchors. Therefore, based on the distance information, various location algorithms can then be applied.

Convex estimation

The convex position algorithm models the known peer to peer communication in the network as a set of geometric constrains. The final location is the solution of a linear optimization

problem which is based on the connectivity and pair-wise angles between nodes. A Linear Problem is a problem of the form:

Minimise: $c^T x$

Subject to: $Ax \leq b$

Bounding-box approach

The bounding-box approach defines a possible area that a node may reside in. This approach based either on distance between the nodes [21] or the radio pattern [22]. (Figure 2.10)

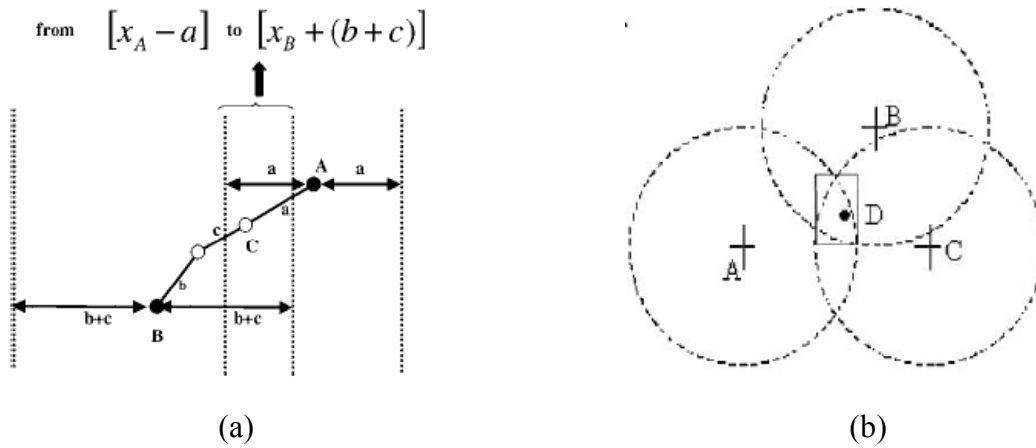


Figure 2.10: Bounding-box examples. (a) Distance-based approach, (b) Radio pattern-based approach

Lateration algorithm

Lateration is a form of triangulation that uses the least square method to estimate particular position from a set of linearised equations in the form of $Ax = b$. Each node gets an estimated distance d_i to the nodes with known position (x_i, y_i) . So the above set of equations can be expressed:

$$\begin{cases} (x_1 - x)^2 + (y_1 - y)^2 = d_1^2 \\ \vdots \\ (x_n - x)^2 + (y_n - y)^2 = d_n^2 \end{cases}$$

The equation $Ax = b$ has

$$A = \begin{bmatrix} 2(x_1 - x) & 2(y_1 - y) \\ \vdots & \vdots \\ 2(x_n - x) & 2(y_n - y) \end{bmatrix} \text{ and } b = \begin{bmatrix} x_1^2 - x_n^2 + y_1^2 - y_n^2 + d_n^2 - d_1^2 \\ \vdots \\ x_{n-1}^2 - x_n^2 + y_{n-1}^2 - y_n^2 + d_n^2 - d_{n-1}^2 \end{bmatrix}, \text{ then } x \text{ can be}$$

estimated by least-square as $x = (A^T A)^{-1} A^T b$.

Probability algorithm

Firstly, in the probability algorithm we record the signal strength with the changing distance. A normal node receives a beacon packet directly from an anchor and it estimates itself to be located on a circular surface centred at that anchor [26]. Each node, after one estimation, adds the ID and the signal strength in the packet and later broadcasts the packet to the neighbours. To estimate its position the normal node processes the cascaded distributions by adding all individual estimates. Finally, after processing the beacon packet, the normal node updates its position by intersecting the new constraints with the current estimates.

Multidimensional scaling method (MDS)

This algorithm used to analyze the dissimilarity of data on a set of objects. The basic MDS-Map algorithm is the following [19]:

1. Compute the shortest paths between all pairs of nodes.
2. Apply classical MDS and use its result in order to construct a relative map.
3. Given sufficient anchor nodes, transform the relative map to an absolute map.

2.3.6 Refinement

The purpose of the refinement process is to adjust the estimated position in the previous step. When one normal node estimates its own position, it informs its neighbors about its possible position. According to the radio communication constraints, the neighboring nodes can adjust their estimates accordingly. After a number of iterations, the position updating becomes small. Then, the nodes can stop the refinement procedure and report their final position [3].

2.3.7 Impact of anchor density

In order to find the impact of anchor density we have to introduce the following relations.

- Anchor deployment density: number of beacons per unit area $\rho = \frac{N}{A}$.

- Anchor per neighbourhood: number of anchors in a normal radio transmission area
 $\mu = \rho \cdot \pi \cdot Range^2$.
- Probability of successful transmission: $p_{success} = p \cdot (1 - p)^\mu$.
- Probability of interference: $p_{interference} = 1 - p_{success}$.

It is obvious that the probability of interference increases exponentially with the anchor per μ . This means that we cannot simply increase the number of anchors in order to maintain higher performance.

2.3.8 Localization Accuracy Metrics

The accuracy of the computed mean square error location is typically evaluated by comparison with the corresponding Cramer-Rao bound (CR bound) [17]. The CR bound gives a lower bound on the error covariance matrix for an unbiased estimate of an estimated parameter.

Other metrics of accuracy are the circular probability (CEP) and geometric dilution of precision (GDOP). The CEP is a function of the error covariance matrix of estimated locations that can be approximated by

$$CEP \cong (3/4)\sqrt{a^2 + b^2}$$

Where a and b are the semimajor axis of the error ellipse. The GDOP measures the effect of the geometric configuration of the reference points on the location estimates and it is defined as the root mean square error in the position estimate and the root mean square distance measurement error.

$$GDOP = \frac{\sqrt{\sigma_x^2 + \sigma_y^2 + \sigma_z^2}}{\sigma_r}$$

2.3.9 Reported precision

The following table presents the experiment results of presented localization algorithms

| Algorithm | Testbed | Nodes | Anchor | Error |
|--------------------|---|-------|------------|------------------------------------|
| Convex Positioning | Not provide similar precision estimation Connectivity can improve precision dramatically | | | |
| Ad hoc Positioning | Isotropic | 100 | 10% 20% | 35% radio range 25% radio range |

| | | | | |
|--------------------------|---|---------|------------|-------------------------------------|
| | Anisotropic | 100 | 10% 20% | 100% radio range 90% radio range |
| N-hop multilateration | 200 different scenarios | 10 -100 | 20% | 27,7 mm |
| Probabilistic approach | 60m x 60m | 5 | 8 | 9,4 – 47% radio range |
| Multidimensional Scaling | Does not specifically provide a quantitative value Algorithm is less dependent on the radio pattern & special terrain topology | | | |

Table 2.2: Reported precision for the positioning algorithms in Ad hoc networks

CHAPTER 3

3.Methodology - Position Estimation

This section describes the proposed algorithm, which is an enhancement of the T. Kamada and S. Kawai method [1], the most popular graph drawing method. Particularly, we introduce a localization framework that is closely linked to the properties of an ad hoc network, compatible with a fully distributed and constantly evolving environment. The proposed algorithm considers a priori and reliability information.

Suppose a network of n nodes. We assume that each node i that joins the network receives the location information of all the other n nodes, in a global 2-D coordinate system, and the accuracy of this location. Thereafter, node i calculates the distance from its neighboring nodes and the accuracy of this distance. There is a variety of measurement techniques that computes the distance between neighboring nodes. In this work, we apply the RSSI model [27], which is the most realistic model for network communication.

Finally, we formulate the localization problem as a constrained least squares problem. The main objective is to find the coordinates of the unlocated node that maximize the sum of the unknown distances under the constraints that all known distances are respected.

3.1 T.Kamada and S.Kawai method

The T.Kamada and S.Kawai method is formulated as an energy optimization problem [4]. It defines an energy or cost function (equation 3.1), based on some virtual physical model of the network. Minimizing this function determines the optimal position of node i that joins the network. In particular, we suppose that the network topology is known and we search for the position X_i to approximate the ideal distance between immediate nodes.

Given a 2-D layout, where node i is placed at point X_i the energy of the system is:

$$E(X) = \sum_{j=1, j \in D^1, i \neq j}^N w_{ij} \cdot \left(\|X_i - X_j\| - d_{ij}(R) \right)^2 \quad (3.1)$$

for a certain node i , where N is the number of nodes in the ad hoc network and D^1 is the set of one-hop neighbors of node i . $X = [x_{ij}]_{n \times 2}$ denotes the estimated locations of the set of n nodes in a 2-dimensional space [1]. $R = [r_{ij}]_{n \times n}$ denotes the ideal distance between the nodes i and j . As already mentioned, the ideal distance $d_{ij}(R)$ between node i and node j can be obtain from the transformation of RSSI values that node i records from beacons received from node j to distance. Beacons are messages broadcasted by every node periodically. The w_{ij} is a $n \times n$ matrix of logical physical values which denotes the weights of the distance between the nodes i and j . The matrices w_{ij} and $R = [r_{ij}]_{n \times n}$ are symmetric.

Local minimization of global energy

We present some definitions for describing the algorithm and outline the method. The position of a node is expressed by x and y coordinates values. Let (x, y) be the coordinates of node X who is applying the location algorithm and (x_i, y_i) be the coordinates of nodes X_i . Then, the energy $E(X)$ is rewritten as follows:

$$E(X) = \sum_{i=1, i \in D^1}^N w_i \cdot \left(\sqrt{(x - x_i)^2 + (y - y_i)^2} - d_i(R) \right)^2 \quad (3.2)$$

If we assume that $A_i = \sqrt{(x - x_i)^2 + (y - y_i)^2}$ when the energy function becomes:

$$E(X) = \sum_i w_i \cdot (A_i - d_i) \quad (3.3)$$

We implement a method of computing a local minimum of $E(X)$ from a certain initial state based on the two-dimensional Newton-Raphson method [1]. The necessary condition of local minimum is:

$$\frac{\partial E}{\partial x} = \frac{\partial E}{\partial y} = 0 \quad (3.4)$$

$$\frac{\partial E}{\partial x} = 2 \sum_i w_i (x - x_i) \left(1 - \frac{d_i}{A_i}\right) \quad (3.5)$$

$$\frac{\partial E}{\partial y} = 2 \sum_i w_i (y - y_i) \left(1 - \frac{d_i}{A_i}\right) \quad (3.6)$$

We can obtain a local minimum which satisfies (3.4) iterating this step. In each step, we choose the solution (x, y) that has the largest value of Δ where:

$$\Delta = \sqrt{\frac{\partial E^2}{\partial x} + \frac{\partial E^2}{\partial y}} \quad (3.7)$$

Starting from $(x^{(0)}, y^{(0)})$ which is equal to the barycentre of the one-hop neighbors of node X the following step is iterating:

$$x^{(t+1)} = x^{(t)} + \delta_x \quad (3.8)$$

$$y^{(t+1)} = y^{(t)} + \delta_y \quad \text{for } t = 0, 1, 2, \dots$$

The unknowns δ_x and δ_y satisfy a pair of linear equations as follows:

$$\frac{\partial^2 E}{\partial x^2}(x^{(t)}, y^{(t)})\delta_x + \frac{\partial^2 E}{\partial x \partial y}(x^{(t)}, y^{(t)})\delta_y = -\frac{\partial E}{\partial x}(x^{(t)}, y^{(t)}) \quad (3.9)$$

$$\frac{\partial^2 E}{\partial y \partial x}(x^{(t)}, y^{(t)})\delta_x + \frac{\partial^2 E}{\partial y^2}(x^{(t)}, y^{(t)})\delta_y = -\frac{\partial E}{\partial y}(x^{(t)}, y^{(t)}) \quad (3.10)$$

The coefficients of above equations (3.9) and (3.10), which are the elements of Jacobian matrix, are computed from the partial derivatives of (3.5) and (3.6) by x and y as follows:

$$\frac{\partial^2 E}{\partial x^2} = 2 \cdot \sum_i w_i \left(1 + \frac{d_i}{A_i} \left(\frac{(x - x_i)^2}{A_i^2} - 1\right)\right) \quad (3.11)$$

$$\frac{\partial^2 E}{\partial x \partial y} = 2 \cdot \sum_i \frac{w_i (x - x_i)(y - y_i) d_i}{A_i^3} \quad (3.12)$$

$$\frac{\partial^2 E}{\partial y \partial x} = 2 \cdot \sum_i \frac{w_i (x - x_i)(y - y_i) d_i}{A_i^3} \quad (3.13)$$

$$\frac{\partial^2 E}{\partial y^2} = 2 \cdot \sum_i w_i \left(1 + \frac{d_i}{A_i} \left(\frac{(y - y_i)^2}{A_i^2} - 1 \right) \right) \quad (3.14)$$

The unknowns δ_x and δ_y can be computed from the (3.9)-(3.14). The iteration (3.8) terminates when the value of Δ at $(x^{(t)}, y^{(t)})$ becomes enough small.

3.2 Weighted Min Max method

Kamada-Kawai approach approximates the ideal position of node X by minimizing the estimated distance between node X and its one-hop neighbors from the ideal one. The weakness of Kamada-Kawai method is that it does not mention all the available information. However, in the Weighted Min Max method we place the unlocated node X close to its one-hop neighbors while maximizing the distance from its not one-hop neighbors. Consequently, Weighted Min Max method observes the full network topology and precisely indicates that if the unlocated node is not one-hop neighbour with another node it is likely that their distance is maximal.

Suppose, the ad hoc network representing in Figure 3.1 that consists of 3 nodes. The red squares define the real position of each node while the green defines the possible position of node 1, the unknown node. Node 1 and 2 are one-hop neighbors, their ideal distance is d , and node 2 is one-hop neighbor with node 3. According to Kamada-Kawai method the possible position of node 1 is one point at the circle with center the coordinates of node 2 and radius d .

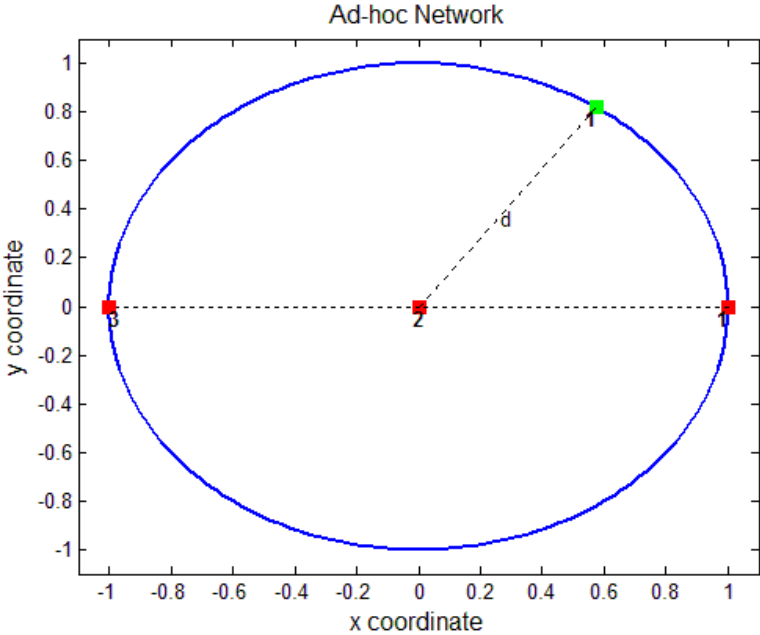


Figure 3.1: Kamada-Kawai method

However, Weighted Min Max method places node 1 at the maximum distance from its nonadjacent nodes. As a result, the possible position of node 1 (Figure 3.2) coincides with the real position.

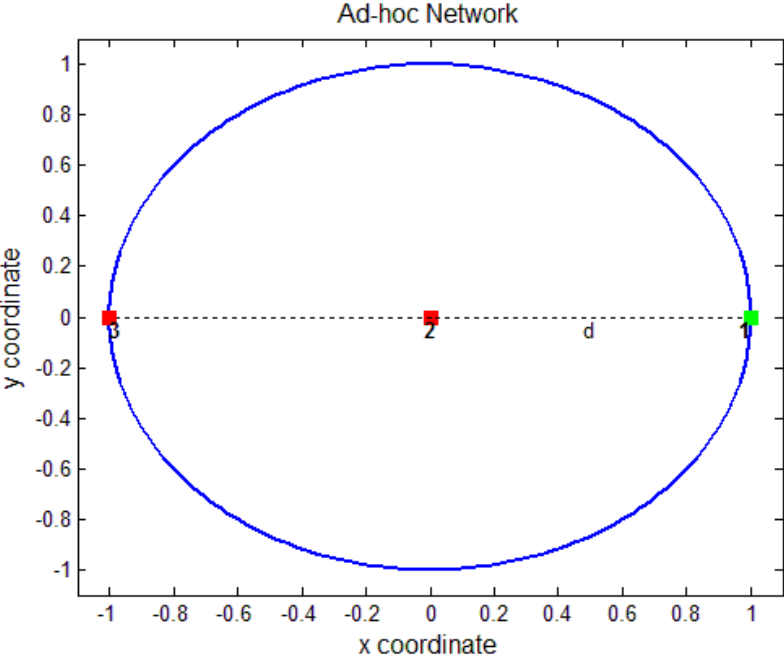


Figure 3.2: Weighted Min Max method

We seek for the position that approximates the ideal distance between adjacent nodes while the sum of the distances from nonadjacent nodes is the maximum. We design the energy function is minimized under these constraints. The function is defined as follows:

$$E(X) = p \cdot \sum_{i=1, i \in D^1}^N w_i \cdot (\|X - X_i\| - d_i)^2 + \frac{1-p}{\sum_{k=1, k \notin D^1}^N v_k \cdot \|X - X_k\|^2} \quad (3.15)$$

where p ($0 \leq p \leq 1$) is physical normalized value, v_k signifies the weights of the distance between the non one-hop neighbors and the unlocated node and d_i is the ideal distance between the unlocated node X and nodes X_i . We presuppose that each node X that joins the network receives the location information of all the other N nodes, in a global 2-D coordinate system and the accuracy of this location.

The coefficient p balances the importance of the distance of the unlocated node from neighboring and non neighboring nodes. When p is closer to 1 more importance is given to the minimization of the difference between the distance of the node X from its one-hop neighbors ($\|X - X_i\|$) and the ideal one (d_i). In the extreme case that $p=1$, the results of the Weighted Min Max method and Kamada-Kawai method are identical. On the other hand, decreasing p , we focus more on the maximization of the distance between node X and its not one-hop neighbors. As a result, we can compute the unknown node location adjusting p based on the uncertainty of the position information of the neighboring nodes.

Derivative computation

We seek for the value X , $X = [x_{ij}]_{n \times 2}$ denotes the estimated locations of the set of N nodes in a 2-D space, where $X = \min E(X)$. In order to find the local minimum of (eq. 3.15) we implement the two-dimensional Newton-Raphson method as represented above. The necessary condition of local minimum is $\frac{\partial E}{\partial X} = 0$. We assume that $A(X) = (\|X - X_i\| - d_i)^2$

and $B(X) = \frac{1}{\|X - X_k\|^2}$. Therefore, the derivative of the energy function is computed as

following:

$$\begin{aligned}
A(X+h) + A(X) &= (\|X - X_i + h\| - d_i)^2 + (\|X - X_i - d_i\|)^2 \\
&\approx \left(\|X - X_i\| \left(1 + h^T \frac{X - X_i}{\|X - X_i\|^2} \right) - d_i \right)^2 + (\|X - X_i - d_i\|)^2 \\
&\approx \left(\|X - X_i\| - d_i + h^T \frac{X - X_i}{\|X - X_i\|} \right)^2 + (\|X - X_i - d_i\|)^2 \\
&\approx 2 \cdot h^T \cdot (X - X_i) \cdot \left(1 - \frac{d_i}{\|X - X_i\|} \right)
\end{aligned} \tag{3.16}$$

$$\begin{aligned}
B(X+h) - B(X) &= \frac{1}{\|X+h - X_k\|^2} - \frac{1}{\|X - X_k\|^2} \\
&\approx \frac{1}{\|X - X_k\|^2} \left(\frac{1}{1 + \frac{2h^T (X - X_k)}{\|X - X_k\|^2}} - 1 \right) \\
&\approx -\frac{1}{\|X - X_k\|^2} \left(\frac{2h^T (X - X_k)}{\|X - X_k\|^2} \right)
\end{aligned} \tag{3.17}$$

Finally according to (3.16) and (3.17)

$$E'(X) = 2p \sum_{i=1, i \in D^1}^N w_i (X - X_i) \left(1 - \frac{d_i}{\|X - X_i\|} \right) - 2(1-p) \sum_{k=1, k \notin D^1}^N v_k \frac{X - X_k}{\|X - X_k\|^4} \tag{3.18}$$

The state satisfying (3.18) equals to zero corresponds to the dynamic state in which node X is located.

3.3 Min Max method

In the Min Max method, like the Weighted Min Max method, we search for the coordinates that minimize the distance from neighboring nodes while non neighboring nodes are placed far apart. The energy function that describes such a layout is defined as follows:

$$E(X) = \frac{\sum_{i=1, i \in D^1}^N w_i (A_i - d_i)^2}{\sum_{k=1, k \notin D^1}^N \|X - X_k\|^2} \quad (3.19)$$

Minimizing eq. 3.19 is useful since it tries to locate adjacent sensors close to each other while separating nonadjacent sensors.

$$\text{Assuming that } A_i = \sqrt{(x - x_i)^2 + (y - y_i)^2} \quad \text{and} \quad B = \sum_{k=1, k \notin D^1}^N (x - x_k)^2 + (y - y_k)^2 \quad (3.19)$$

becomes:

$$E(X) = \frac{\sum_{i=1, i \in D^1}^N w_i \cdot (A_i - d_i)^2}{B} = \sum_{i=1, i \in D^1}^N w_i \cdot E_i(X) \quad (3.20)$$

$$\text{Where: } E_i(X) = \frac{(A_i - d_i)^2}{B}$$

In order to find the local minimum of (3.19) we implement the two-dimensional Newton-Raphson method as above.

Derivative computation

Thus, the coefficients in order to solve the linear equations (3.9) and (3.10) are the following:

$$\frac{\partial E_i}{\partial x} = \frac{2(A_i - d_i) \left(\frac{x - x_i}{A_i} \right) B - (A_i - d_i)^2 C_x}{B^2} \quad (3.21)$$

$$\frac{\partial E_i}{\partial y} = \frac{2(A_i - d_i) \left(\frac{y - y_i}{A_i} \right) B - (A_i - d_i)^2 C_y}{B^2}$$

$$\text{If } Numx = 2(A_i - d_i) \left(\frac{x - x_i}{A_i} \right) B - (A_i - d_i)^2 C_x, \quad Numy = 2(A_i - d_i) \left(\frac{y - y_i}{A_i} \right) B - (A_i - d_i)^2 C_y$$

and $Den = B^2$ the partial derivatives of (3.21) by x and y are as follows:

$$\frac{\partial^2 E_i}{\partial x^2} = \frac{1}{B^4} \left(\frac{\partial Numx}{\partial x} \cdot Den - Numx \cdot \frac{\partial Den}{\partial x} \right)$$

$$\frac{\partial^2 E_i}{\partial y^2} = \frac{1}{B^4} \left(\frac{\partial Num_y}{\partial y} \cdot Den - Num_y \cdot \frac{\partial Den}{\partial y} \right)$$

$$\frac{\partial^2 E}{\partial x \partial y} = \frac{1}{B^4} \left(\frac{\partial Num_x}{\partial x} \cdot Den - Num_x \cdot \frac{\partial Den}{\partial x} \right)$$

$$\frac{\partial^2 E}{\partial y \partial x} = \frac{1}{B^4} \left(\frac{\partial Num_y}{\partial x} \cdot Den - Num_y \cdot \frac{\partial Den}{\partial x} \right)$$

Where:

$$\frac{\partial Num_x}{\partial x} = 2 \left(\left(\frac{x-x_i}{A_i} \right)^2 B + (A_i - d_i) \frac{A_i - \frac{(x-x_i)^2}{A_i}}{A_i^2} B + (A_i - d_i) \left(\frac{x-x_i}{A_i} \right) C_x \right) - 2(A_i - d_i) \frac{x-x_i}{A_i} C_x - 2K(A_i - d_i)^2$$

$$\frac{\partial Den}{\partial x} = 2BC_x$$

$$\frac{\partial Num_y}{\partial y} = 2 \left(\left(\frac{y-y_i}{A_i} \right)^2 B + (A_i - d_i) \frac{A_i - \frac{(y-y_i)^2}{A_i}}{A_i^2} B + (A_i - d_i) \left(\frac{y-y_i}{A_i} \right) C_y \right) - 2(A_i - d_i) \frac{y-y_i}{A_i} C_y - 2K(A_i - d_i)^2$$

$$\frac{\partial Den}{\partial y} = 2BC_y$$

$$\frac{\partial Num_x}{\partial y} = 2 \left(\left(\frac{y-y_i}{A_i} \right) \left(\frac{x-x_i}{A_i} \right) B - (A_i - d_i) \frac{(x-x_i)(y-y_i)}{A_i^3} B + (A_i - d_i) \left(\frac{x-x_i}{A_i} \right) C_y \right) - 2(A_i - d_i) \frac{y-y_i}{A_i} C_x$$

$$\frac{\partial Num_y}{\partial x} = 2 \left(\left(\frac{y-y_i}{A_i} \right) \left(\frac{x-x_i}{A_i} \right) B - (A_i - d_i) \frac{(x-x_i)(y-y_i)}{A_i^3} B + (A_i - d_i) \left(\frac{x-x_i}{A_i} \right) C_y \right) - 2(A_i - d_i) \frac{y-y_i}{A_i} C_x$$

Where:

$$C_x = 2 \cdot \sum_{k=1, k \neq D}^N (x-x_k) \quad C_y = 2 \cdot \sum_{k=1, k \neq D}^N (y-y_k)$$

K : is the number of not one hop neighbors of node X .

3.4 RSSI model

In this subsection we present the RSSI propagation model we use in order to find the ideal distance between adjacent nodes.

Among the several models proposed for estimating the distance between a node l and its one-hop neighbors, the most realistic and commonly used one is the *received signal strength indicator* (RSSI) model [27]. In this model, node i broadcasts signal to all its one-hop neighbors and they can estimate the distance between them and the node l on the basis of the signal they receive. We suppose that the estimated position of node l is (x, y) and the positions of its i one-hop neighbors are (x_i, y_i) .

The commonly accepted transmission model expresses the received power p_i (in dBm) as:

$$p_i = p_0 + 10n \log\left(\frac{d_i}{d_0}\right) \quad (3.22)$$

where p_0 is the received power in dBm at a reference distance d_0 and n is the path loss exponent which is a constant depending on the transmission medium (indoors, outdoors) and ranges typically from 2 to 4. In some environments, such as buildings, stadiums and other indoor environments, the path loss exponent drops below to 2 [27].

If the received power in mW at the point k is P_k , and $P_{k'}$ is the received power at some reference point k' , then the received power p_k in dBm at point k is defined as:

$$p_k = 10 \log\left(\frac{P_k}{P_{k'}}\right) \quad (3.23)$$

The measured power, however, differs from that given in Equation (3.22); due to channel fading (variation of the received signal power caused by changes in transmission medium or path), the measured power is $\hat{p}_i = p_i + x$. The random variable x represents the medium-scale channel fading and is typically modeled as Gaussian zero-mean with variance σ^2 (in dBm). Typically, σ is as low as 4 and as high as 12 (this implies that the error may be large). Inserting \hat{p}_i and \hat{d}_i into (3.22), we get:

$$\hat{p}_l = p_0 + 10n \log\left(\frac{\hat{d}_l}{d_0}\right) \quad (3.24)$$

where now the measured power \hat{p}_l in dBm relates to the measured distance \hat{d}_l by node l . By combining the above equations, we get that the relation between the measured distance and the actual distance is:

$$\log \hat{d}_l = \log d_l + \frac{x}{10n} \quad (3.25)$$

$$\hat{d}_l = d_l \cdot 10^{\frac{x}{10n}} \quad (3.26)$$

CHAPTER 4

4. Evaluation

In this Chapter we study the performance of the localization methodologies Kamada-Kawai, Weighted Min Max and Min Max at the same scenario. We demonstrate the improvement of the Kamada-Kawai method by adding the information of the nonadjacent nodes. Additionally, we present the performance of the Weighted Min Max method using different coefficient values.

At the second section of this Chapter we describe the network generator used for simulations. Moreover, we evaluate the accuracy of the Weighted Min Max process under a specific sensor deployment strategy in different environments. We measure the sensitivity of the algorithm to noise in the distance measurements and in the known position of each node. The *final location error* is the Euclidean distance between the estimated position of the unlocated node and the real one.

4.1 Performance analysis

We implement the Kamada-Kawai method (Figure 4.1) and the Weighted Min Max method (Figure 4.2) in an ad hoc network of 3 nodes. At the following figures the one-hop neighbors are connected through a line, the red squares represent the true position of the node, while the green represent the estimated position of node 1 at each iteration of Newton-Raphson method. Finally, the violet circle represents the transmission range of the corresponding node. The initial point at the Newton-Raphson method is $(0, 1)$. Figure 4.1 demonstrates the contour diagram of Energy function 3.1 and Figure 4.2 the contour diagram of Energy

function 3.15. At the following contour diagrams the blue colour represents the lower value of the Energy function while the red colour represents the maximum.

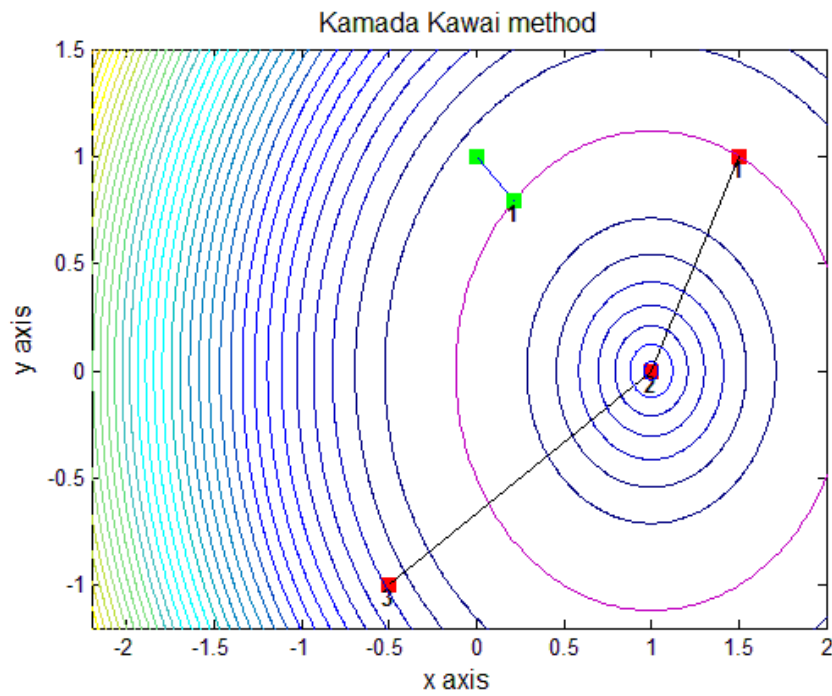


Figure 4.1: Kamada Kawai method in a network of 3 nodes.

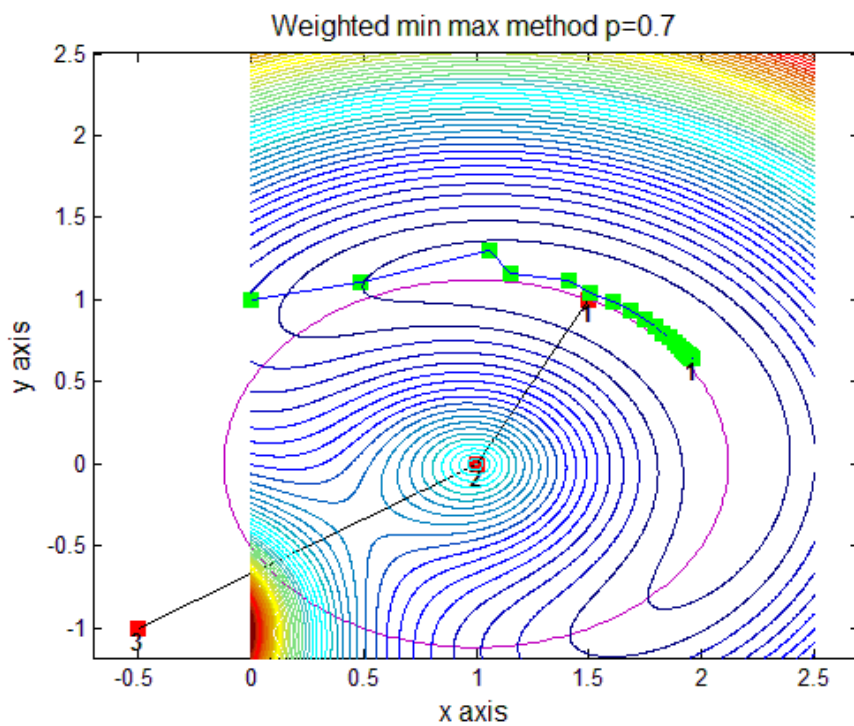


Figure 4.2: Weighted Min Max method in a network of 3 nodes.

According to Kamada-Kawai method the possible position of node 1 is one point of the circle with centre the position of node 2 and radius the distance between them (1 unit). Nevertheless, the Weighted Min Max method exploits the fact that nonadjacent nodes should be placed far apart. This means that we seek for the optimal position for the node 1 while respecting the unknown distances. As a result, if we apply the Weighted Min Max method with $p=0.7$ (Figure 4.2) we observe that the final position of node 1 is the point of the circle, with centre the position of node 2 and radius the distance between them, which has the maximum distance from node 3 (its not one-hop neighbour).

Moreover, the final position error of node 1 decreases while the number of its one-hop neighbour increases (Figure 4.3). In fact, a large number of neighbours will improve the quantity of the results.

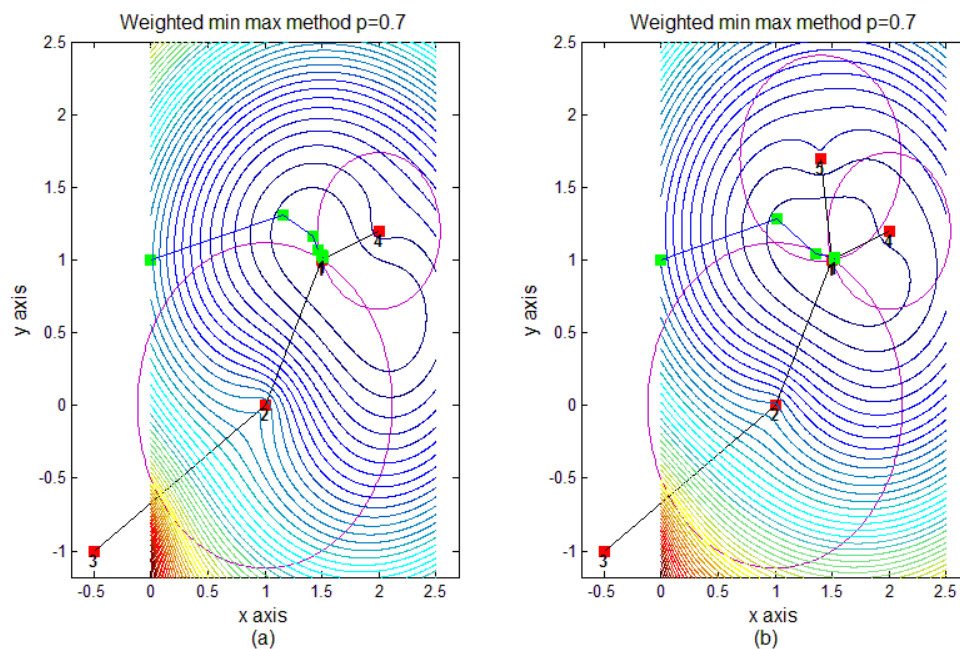


Figure 4.3: Weighted Min Max method in a network of 4 and 5 nodes, respectively

We employed the methods described in Chapter 3, at the following Ad hoc network (Figure 4.4). The initial point of the Newton-Raphson method set $(-1, 3)$.

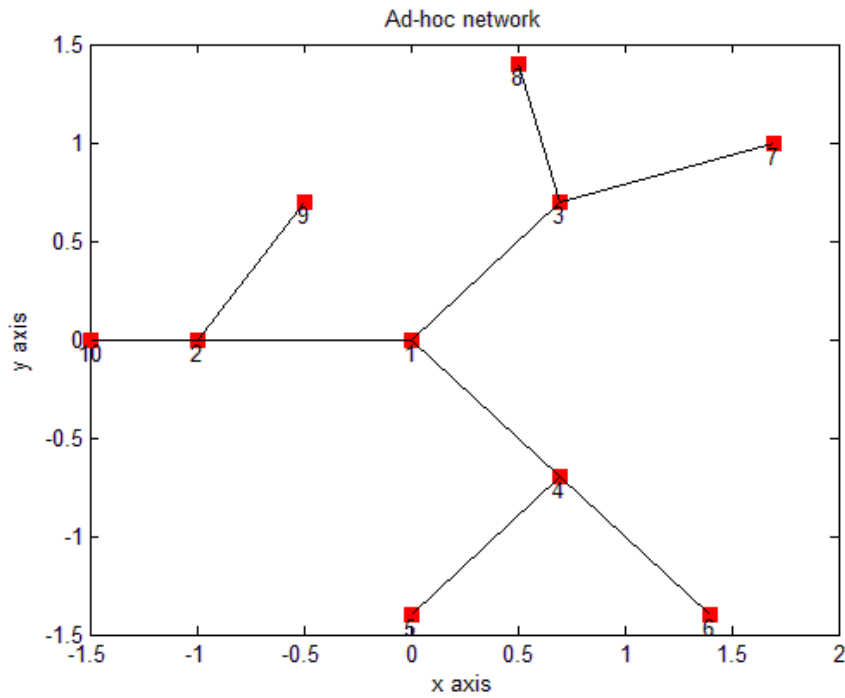


Figure 4.4: Network topology

Figure 4.5 demonstrates the results of Kamada Kawai method. The final position of node 1 matches with the real one.

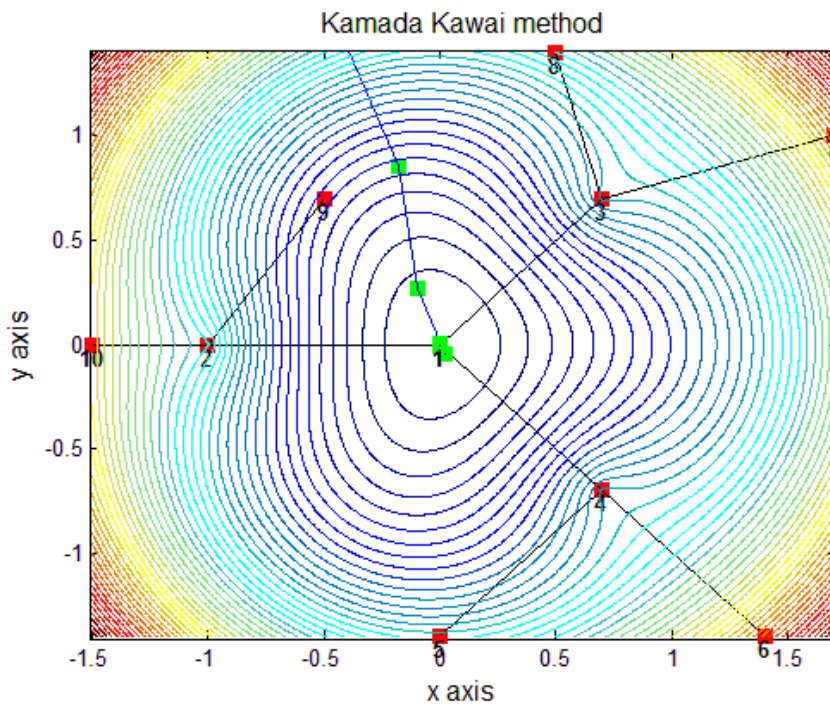


Figure 4.5: Kamada Kawai method in a network of 10 nodes. Node 1 implements the localization algorithm

Figure 4.6 shows the contour diagrams of the Energy function 3.15. It illustrates the results of the Weighted Min Max method when $p = 0.9, p = 0.5, p = 0.1, p = 0.01$. We observe that decreasing p we focus on maximizing the distances (equation 3.15) between node 1 and its not one-hop neighbors. At the extreme case where $p=0.01$ (Figure 4.6) we remark that the unknown node elongates from its not one-hop neighbors. In this example, the weight given to the minimization of the difference between the ideal distance from the one-hop neighbors and the estimated tends to zero.

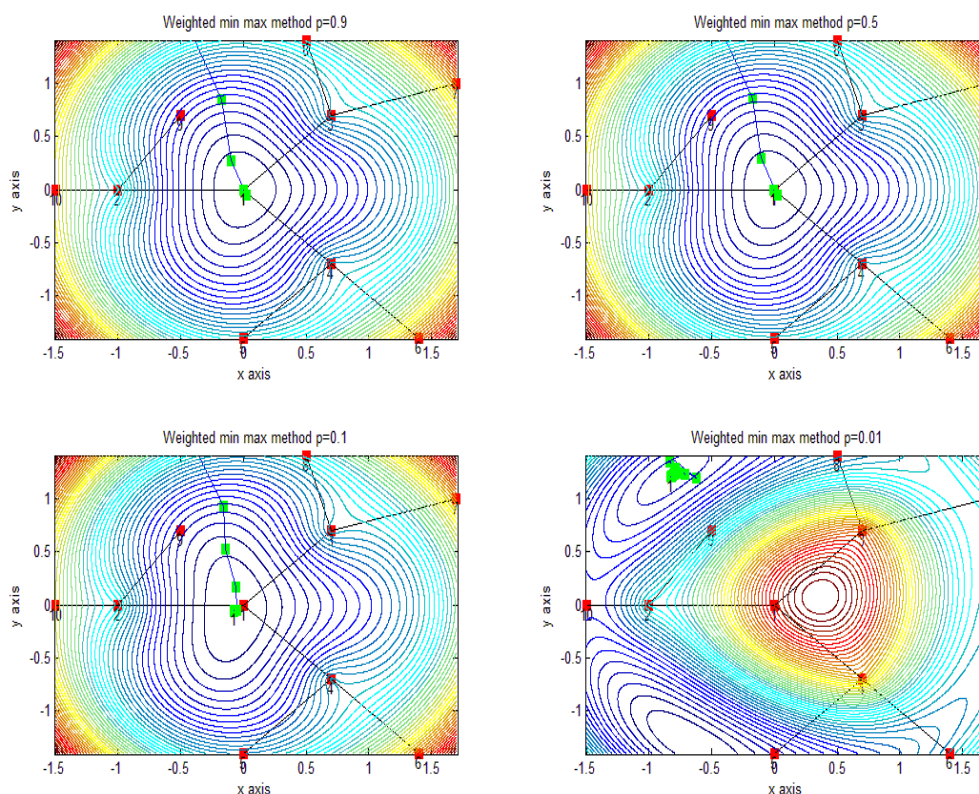


Figure 4.6: Weighted Min Max method in a network of 10 nodes. Node 1 implements the localization algorithm

Figure 4.7 represents the contour diagram of the Energy function 3.19 and demonstrates the results of the Min Max method.

The Min Max and the Weighted Min Max method satisfy the same constraints. However, we observe that when the sum of the not one-hop neighbor's distances tends to zero ($\sum_{k=1, k \notin D_1}^N \|X - X_k\|^2$) the Energy function 3.19 of the Min Max method tends to infinity. Additionally, the Weighted Min Max method prunes the cases where the unknown value tends to infinity. Consequently, for the reasons mentioned above we evaluate the performance of the Weighted Min Max localization algorithm via simulations in real-world conditions.

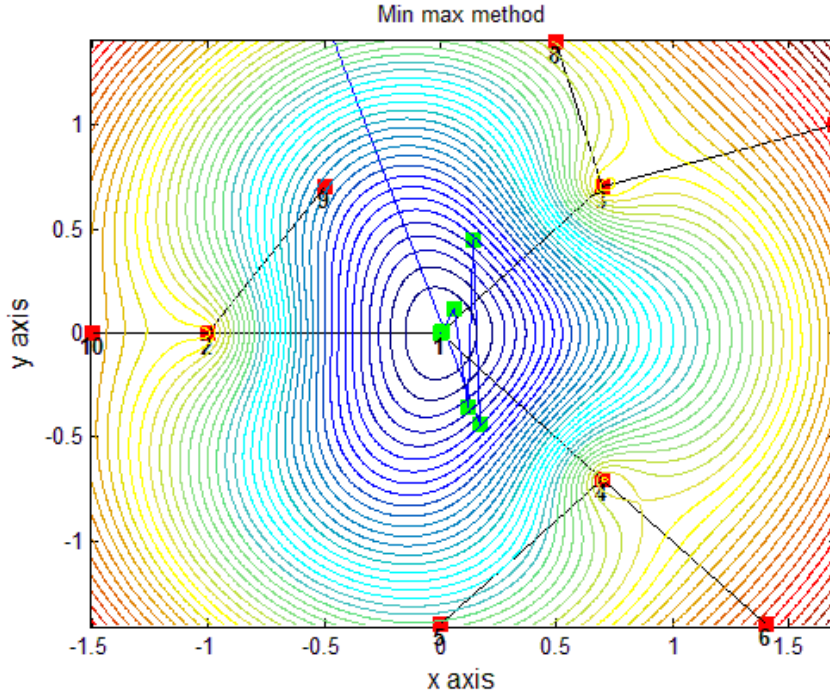


Figure 4.7: Min Max method in a network of 10 nodes. Node 1 implements the localization algorithm

4.2 Network Generator- Simulations

In this subsection we portray the network generator used for the simulations. Moreover, we evaluate the accuracy of the localization process based on the measurement noise parameters under a specific scenario in different environments. The simulations are implemented in MATLAB [31].

Network Generator

We suppose that n nodes n_1, n_2, \dots, n_n are randomly placed in a 1000 by 1000 square meters region and the average radio range is 100(m). Sensors have the same maximum radio range. Each node at the ad hoc network has a known position X_i with coordinates (x_i, y_i) , for $i = 1 \dots n$. Each node s that joins the network receives beacons from its k one-hop neighbors and run the position estimation algorithm in order to be located. The one-hop neighbors of node s transmit information about their location with a signal of normalized intensity to

node s that does not know its location. Based on the locations of the nodes at the ad hoc network and the estimated distances from its one-hop neighbors the node s is to compute its actual position (Figure 4.8).

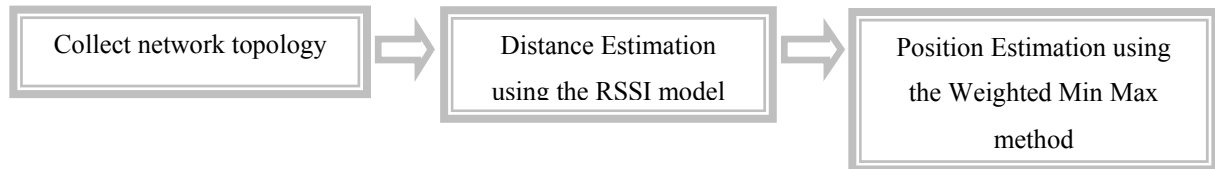


Figure 4.8: Schema of simulation

Each node broadcasts to its one-hop neighbors:

1. An estimation of its position in a global 2-D coordinate system.
2. An indicator of the location algorithm used in order to be located.
3. A location error variance different for each localization method.

Particularly, the indicator of the localization method is:

- 1 → for very rough estimate, ex: If the position information is that the node is near to Seine.
- 2 → for estimations based on a localization algorithm.
- 3 → for estimated based on GPS technology.
- 4 → when the node is a fixed node.

The location error variance for each method is:

- 50 meters for rough estimate.
- 10 meters for a localization algorithm.
- 5 meters for GPS technology.
- 0 meters for a fixed node.

In our simulations node 1, runs the Weighted Min Max method in order to be located. We consider two different errors.

1. The errors of neighboring sensor distance estimation (δ_i) using the RSSI model. The measurement error is a zero-Gaussian random variable with variance σ_i^2 (in dBm).
2. The final location error of each sensor in the network. The location error is a zero-Gaussian random variable with variance σ^2 (in meter). If the position of a node is X_i and the error is ξ_i then the estimated position is $\hat{X}_i = X_i + \xi_i, i = 1 \dots n$. The location error ξ_i depends on the localization algorithm that each node applies.

Simulations

We test the performance of our approach in a specific node development strategy (Figure 4.9). Node 1, the unlocated node, is running the positioning algorithm. Especially, Table 4.1 represents the localization technique of each node. The neighboring relation between the nodes is demonstrated via a line.

| Node | Method | Method indicator |
|-------|------------------------|------------------|
| 2,6,8 | Rough estimation | 1 |
| 5,10 | Localization algorithm | 2 |
| 4,9 | GPS | 3 |
| 3,7 | Fixed node | 4 |

Table 4.1: Data of the Ad hoc network that consists of 10 nodes.

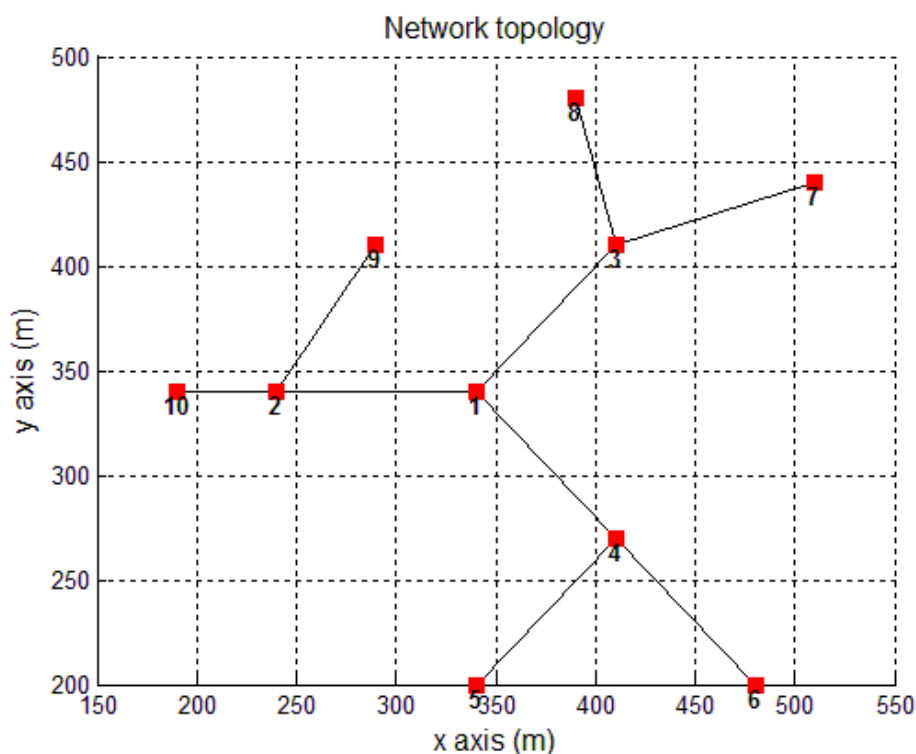


Figure 4.9: Network topology

The weights at the energy function 3.15 are $w_i = \frac{1}{\sigma_i^2} + \frac{1}{\xi_i^2}$ and $v_k = \frac{1}{\xi_k^2}$ and $p=0.7$. The value n at equation (3.22) is equal to 3. Finally, the violet circles represent the estimation position error.

Figure 4.10 and Figure 4.11 demonstrate the results of the Weighted Min Max method for different measurement errors. Figure 4.10 presents an ad hoc network when the mean location error, due to the positioning algorithm, is 11.1392 (m) and the mean error of neighboring sensor distance estimation is 44.6726 (m). Moreover, Figure 4.11 shows the results at the same network when the mean location error, due to the positioning algorithm, is 6.5114 (m) and the mean error of neighboring sensor distance estimation is 73.7992 (m). At the first experiment the final location error of node 1 is 19.1613 (m) and at the second is 49.9477 (m).

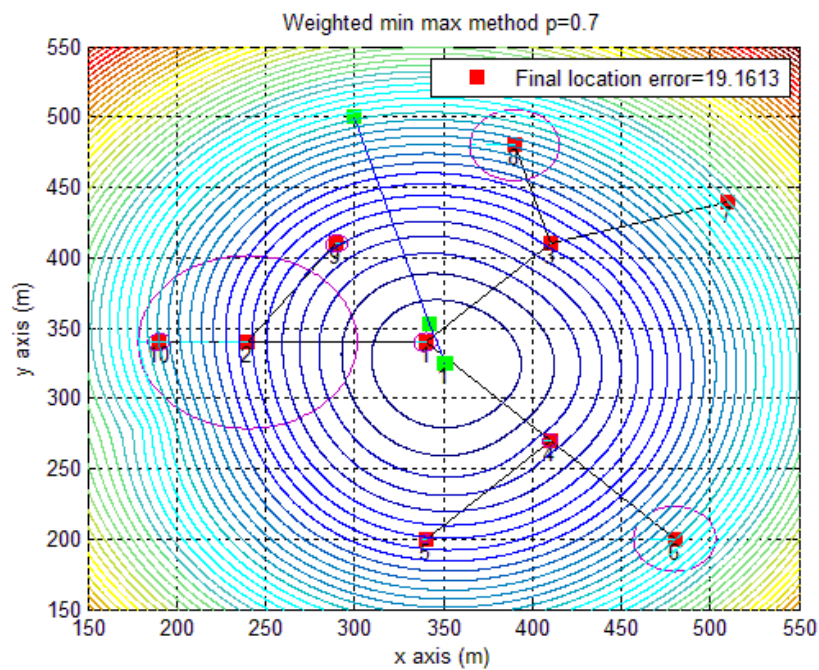


Figure 4.10: Weighted Max Method. The final location error is 19.1613 (m).

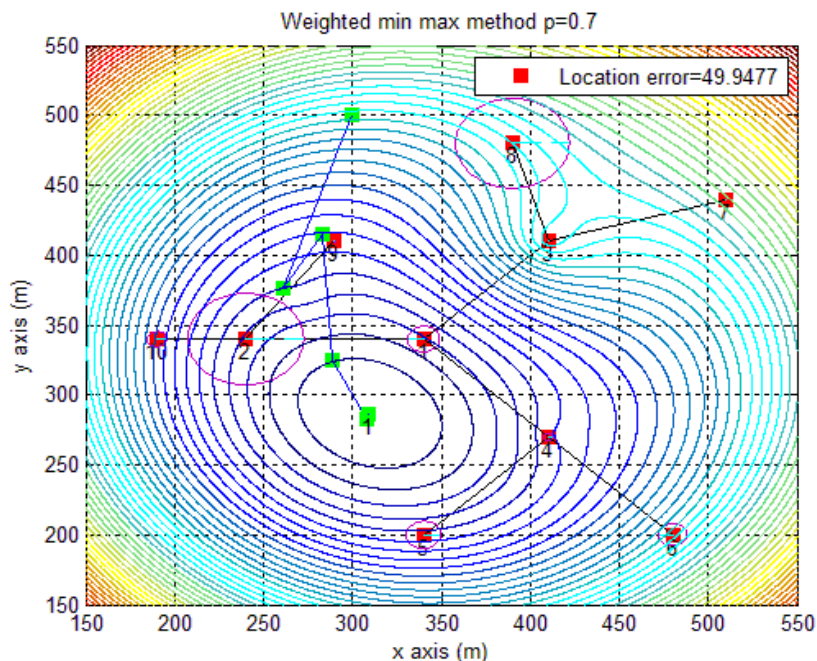


Figure 4.11: Weighted Max Method. The final location error is 49.9477 (m)

It seems that the key to successful results is the minimization of the measurement errors.

In order to test the accuracy of our algorithm we have tested Weighted Min Max method 100 times at the same sensor deployment strategy (Figure 4.9), in different environments. Figure 4.12 demonstrate the location error of the sensors in the network. Particularly, we applied our algorithm for different values of n . According to the RSSI model (equation 3.30), n is the path loss exponent which is a constant depending on the transmission medium (indoors, outdoors) and ranges typically from 2 to 4. In some environments, such as buildings, stadiums and other indoor environments, the path loss exponent drops below to 2. Figure 4.13(a) presents the accuracy of the Weighted Min Max location error and Figure 4.13(b) shows the error of the Euclidian distance due to RSSI measurements.

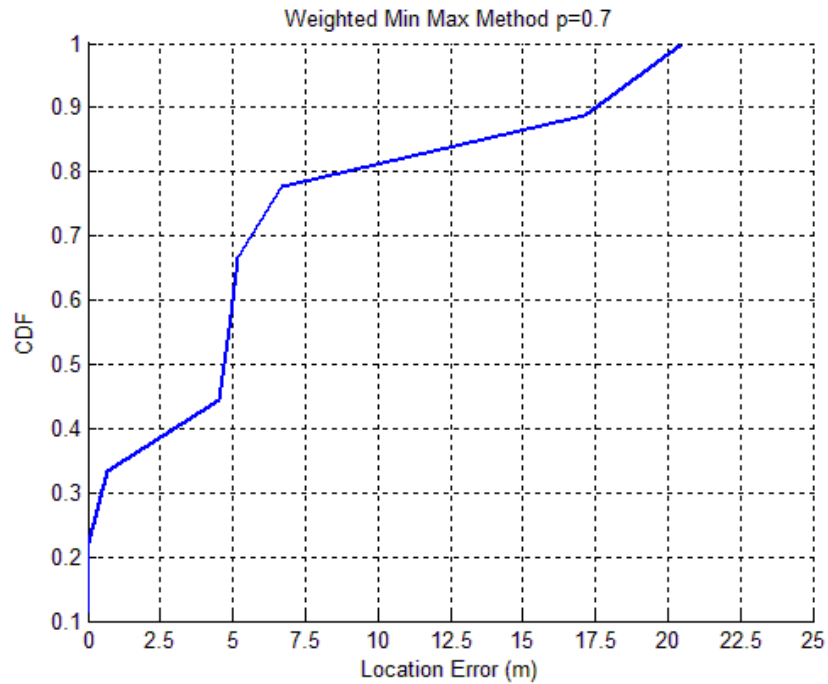


Figure 4.12: Location error of the sensors in the network at figure 4.9. The error depends on the Location algorithm each node runs.

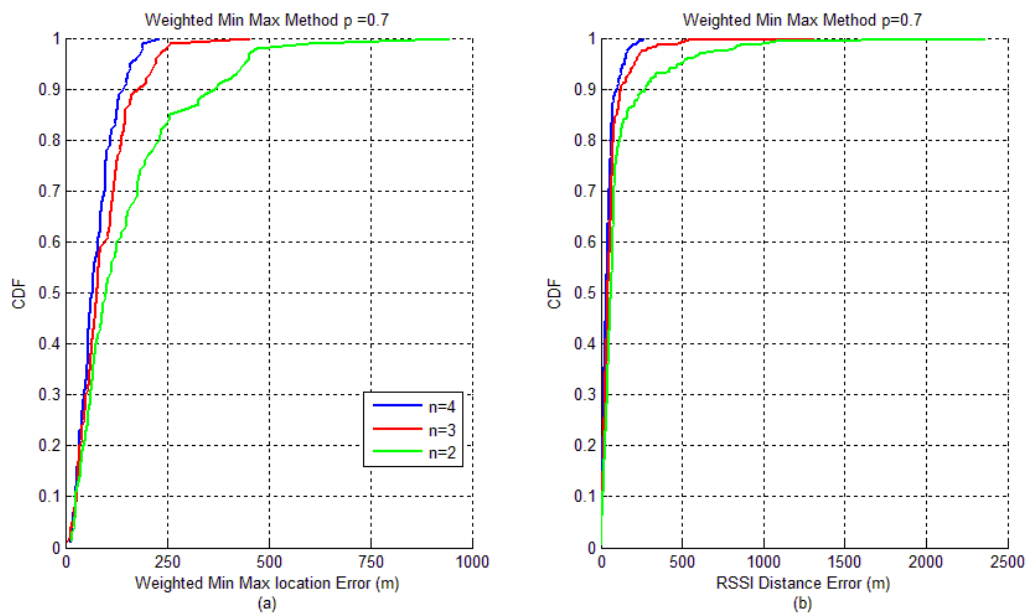


Figure 4.13: (a) Weighted Min Max location error (m). (b) Error of the Euclidian distance due to RSSI measurements for different values of path loss exponent.

Moreover, we observe the accuracy of the Weighted Min Max method in indoor environments, $n=1.5$. Table 4.2 represents the localization technique of each node and Figure 4.14 shows the location error of the nodes.

| Node | Method | Method indicator |
|----------|------------------------|------------------|
| 2,6,8 | Rough estimation | 1 |
| 5,10,4,9 | Localization algorithm | 2 |
| 3,7 | Fixed node | 4 |

Table 4.2: Data of the Ad hoc network that consists of 10 nodes.

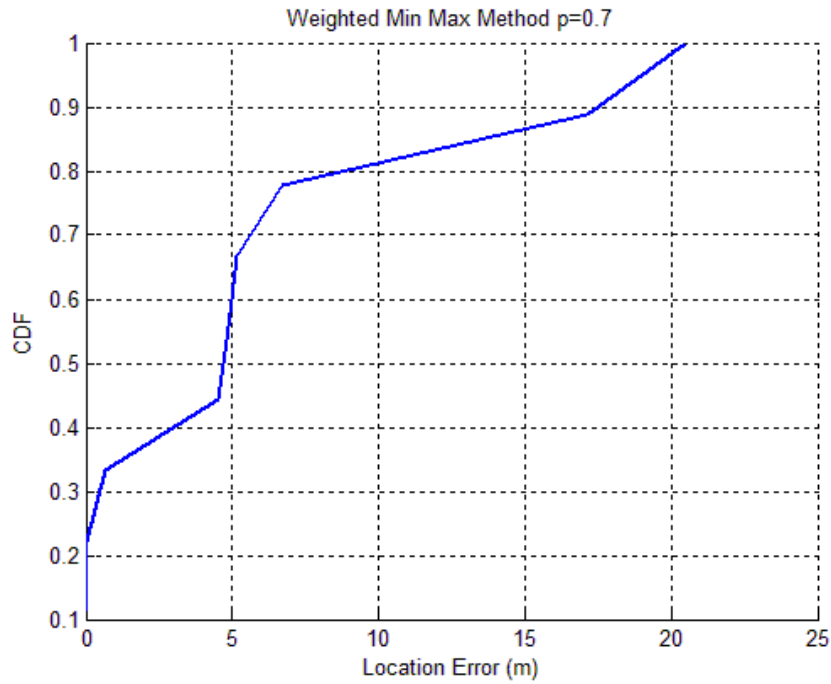


Figure 4.14: Location error of the sensors in the network at fig. 4.9. The error depends on the Location algorithm each node runs.

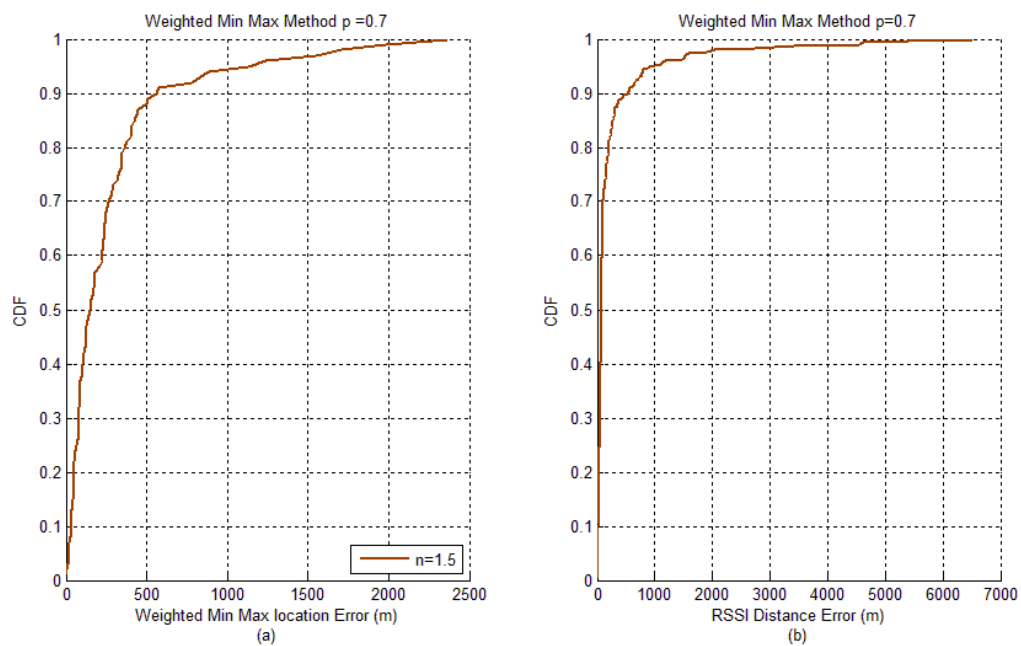


Figure 4.15: (a) Weighted Min Max location error (m). (b) Error of the Euclidian distance due to RSSI measurements for different values of path loss exponent.

| Path loss value | Median WMM Location Error (m) | Median RSSI Distance Error (m) |
|-----------------|-------------------------------|--------------------------------|
| n=1.5 | 148.8528 | 77.3759 |
| n=2 | 100.3591 | 62.0955 |
| n=3 | 78.3765 | 43.0869 |
| n=4 | 66.6663 | 34.3428 |

Table 4.3: Localization performance of the Weighted Min Max (WMM) method in 4 different environments.

The RSSI is environment dependent, moreover in indoor environments the wireless channel is very noisy and the radio frequency signal can suffer from reflection, diffraction and multipath effect. As a result the signal strength becomes a complex function of distance. As expected, Figure 4.13(a) shows that the higher the path loss exponent, the lower location error the algorithm returns. Table 4.3 portrays the results explicitly for every different environment. The accuracy is lower in indoor environments (Figure 4.15).

CHAPTER 5

5. Received Signal Strength Indicator

The existence of radio connectivity and the attenuation of radio signal with distance are attractive properties that could potentially be exploited to estimate the positions of wireless devices. The Received Signal Strength Indication (RSSI) has attracted a lot of attention in the recent literature for obvious reasons. The RSSI eliminates the need for additional hardware in small wireless devices, and exhibits favorable properties with respect to power consumption, size and cost.

The RSSI is a measurement of the strength (not necessarily the quality) of the received signal in a wireless network, in arbitrary units, depending on the hardware (i.e., wireless card) used. Location-sensing techniques that using the received signal strength, also uses a known mathematical model which describes the path loss attenuation of the signal with distance. The measurement of signal strength provides distance estimation between the mobile object and the base station.

In order to test the correlation of the RSSI measurements and the distance we collected a number of measurements both in an indoor and an open-field environment. In this chapter we present the experiments.

5.1 Measurements

5.1.1 Outdoor environment

In order to test the impact of the distance and the signal strength measurements we performed the following experiment. In an open air environment at the 'Parc Mousouris' we took peer to

peer signal strength measurements from two peers. The characteristics of the two peers shown in the following table:

| Machine | Characteristic | Role |
|---------|---|--------|
| NEC2 | Name: adhoc-nec2 Operating system: Ubuntu 8.10, noyau 2.6.27-11-generic Wireless card: Atheros AR5212/AR5213 | Mobile |
| NEC3 | Name: adhoc-nec3 Operating system: Ubuntu 8.10, noyau 2.6.27-11-generic Wireless card : Atheros AR5212/AR5213 | Fix |

Table 5.1: Characteristics of the nodes used in the outdoor experiment

The red square at following figure describes the testbed area.



Figure 5.1: Testbed area ‘Parc Montsouris’. The experiments took place at the red square.

We started the measurements with no distance between the peers. During the experiment the first peer was stable while the second was moving. Every two meters we collected 100 measurements of signal strength in order to observe the distribution of the signal strength. The maximum distance between peers was 78 meters.

Figure 5.2 shows all the 100 signal strength values collected every 2 meters.

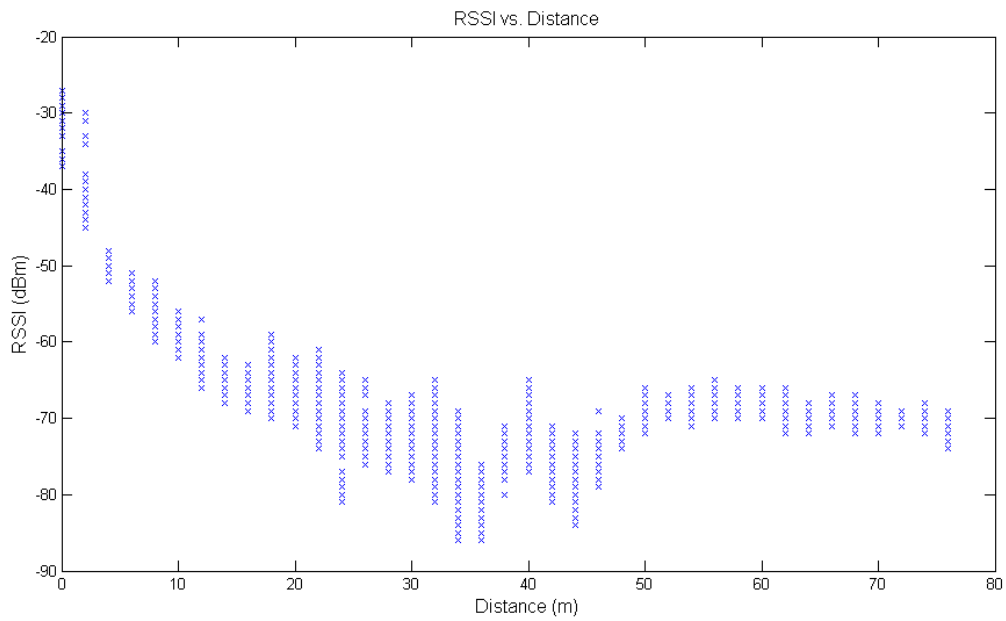


Figure 5.2: RSSI measurements from the outdoor experiment in ‘Parc Montsouris’

The following figure depicts the RSSI values recorded at different distances between the receiver and the transmitter.

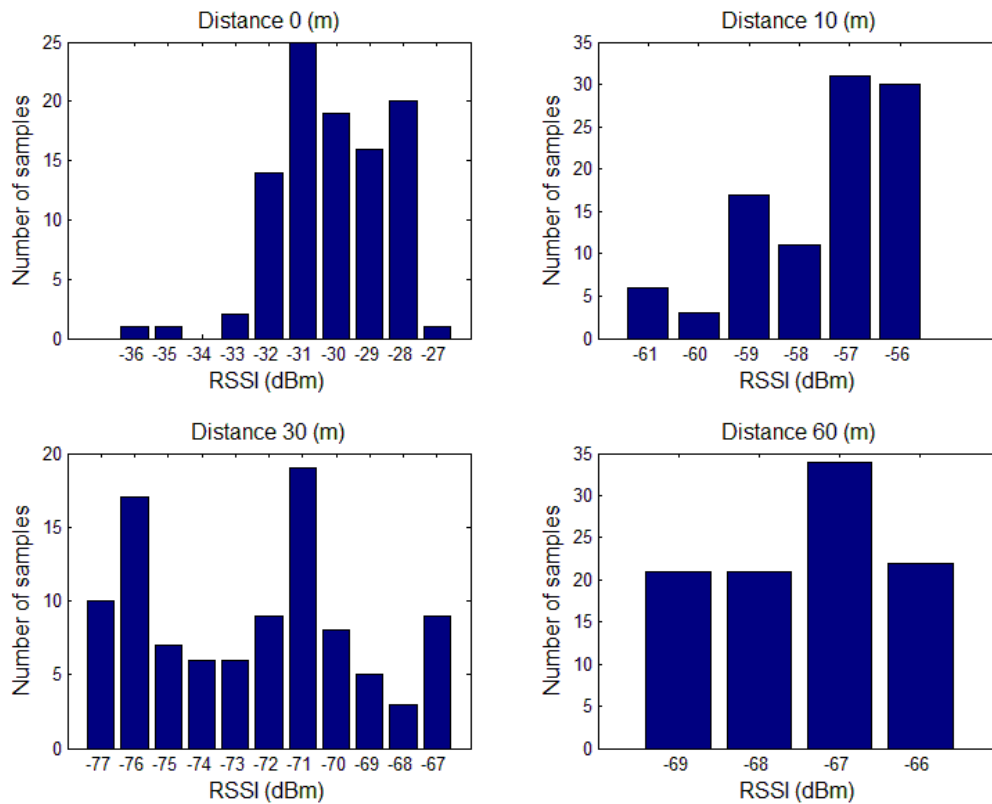


Figure 5.3: RSSI variability

Figure 5.4 illustrates the median and the mean values of the signal strength measurements shown at the Figure 5.2. We observe that there are not outliers.

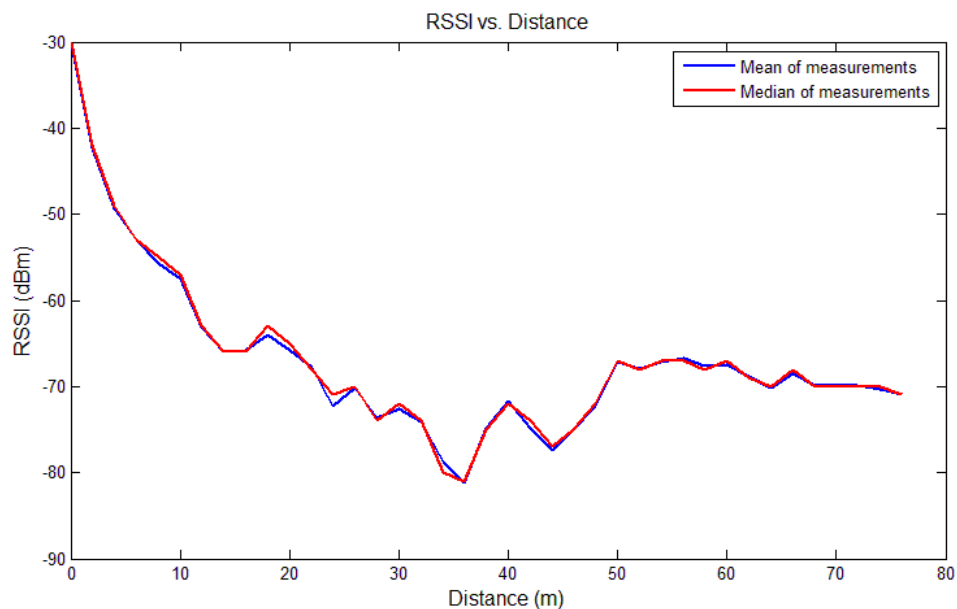


Figure 5.4: RSSI comportment at an outdoor environment

We notice that as the distance between peers increases the signal-strength value decreases, as expected. Though, there are points were in slightly longer distances, the signal strength is higher. This could be the result of a sudden change - decrease of the density of user, which happens often in this testbed, due to the fact that people move in the area. Finally, another reason for this phenomenon is the physiology of the testbed (such as trees and statues) which is the factor with the highest impact on the signal strength along with the density of users.

5.1.2 Indoor environment

In order to test the impact of the distance and the signal strength measurements, in an indoor environment, we did the following experiment.

In a testbed area of 11m x 8m = 88m² at the Institute of Computer Science (ICS), FORTH (Foundation for Research and Technology, Hellas) we took peer to peer signal strength measurements from two peers. The characteristics of the two peers are shown at the following table.

| Machine | Characteristic | Role |
|---------|---|--------|
| Vaio | Name: adhoc-vaio Operating system: Linux – Ubuntu 7.04, released in April 2007 Wireless card: ipw2200 | Mobile |
| Toshiba | Name: adhoc-tosh Operating system: Ubuntu Linux – Ubuntu 7.04, released in April 2007 Wireless card ipw2200 | Fix |

Table 5.2: Characteristics of the nodes used in the indoor experiment.

The conditions were normal (5 persons in the testbed area).The green square at following figure shows the floor plan of the testbed area.

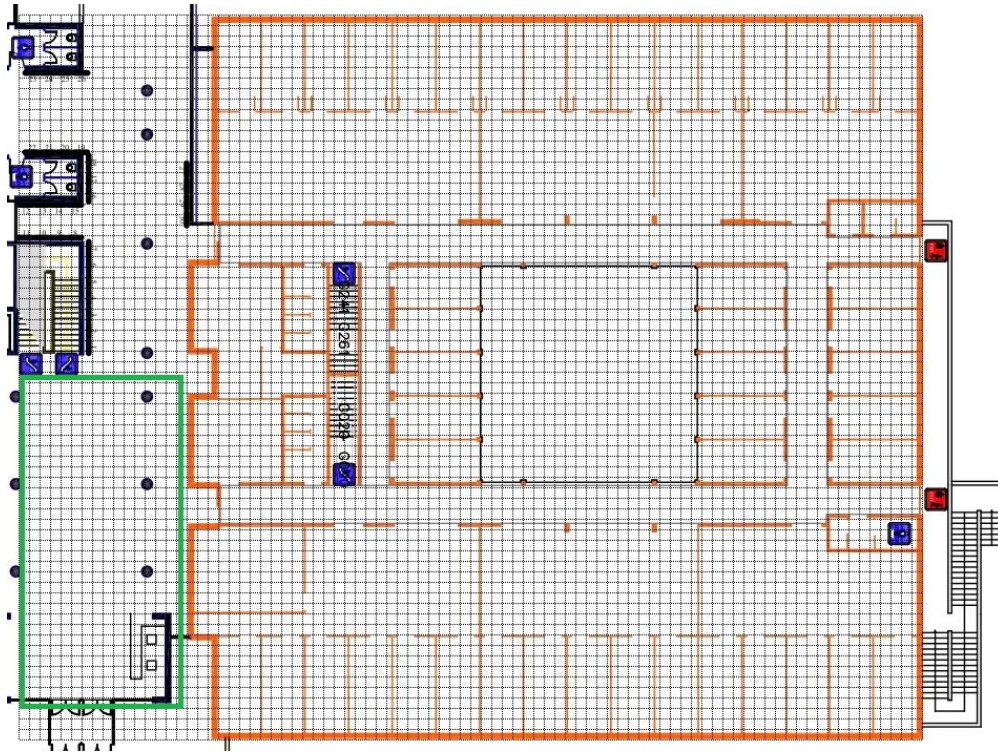


Figure 5.5: Floor plan of the testbed area ICS-FORTH. The experiments took place at the green square

We took the measurements started with the 2 peers the one next to the other (distance=0). During the experiment the one peer was stable while the other was moving. Every one meter we took 60 measurements in order to observe the distribution of the signal strength. The maximum distance between was 13 meters. As we were expected the variability of signal strength values increases in indoor environments (Figure 5.6). In case of inner spaces, reflections become the main problem in performing RSSI distance prediction [28]. The randomness that the reflections introduce in the RSSI values can be seen at Figure 5.7.

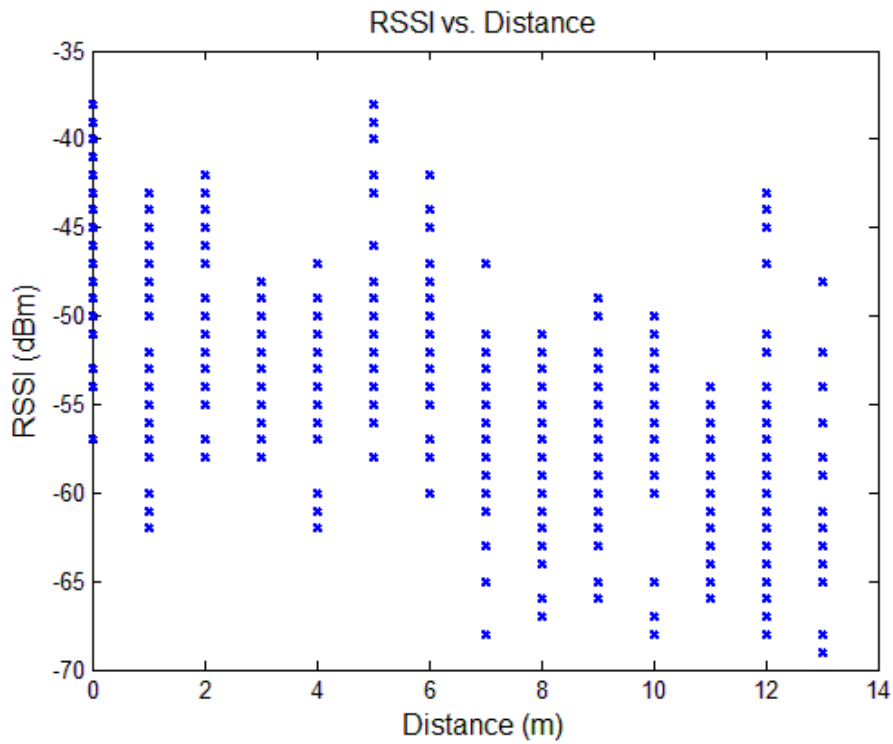


Figure 5.6: 60 RSSI measurements collected every one meter during the experiment in ICS-FORTH.

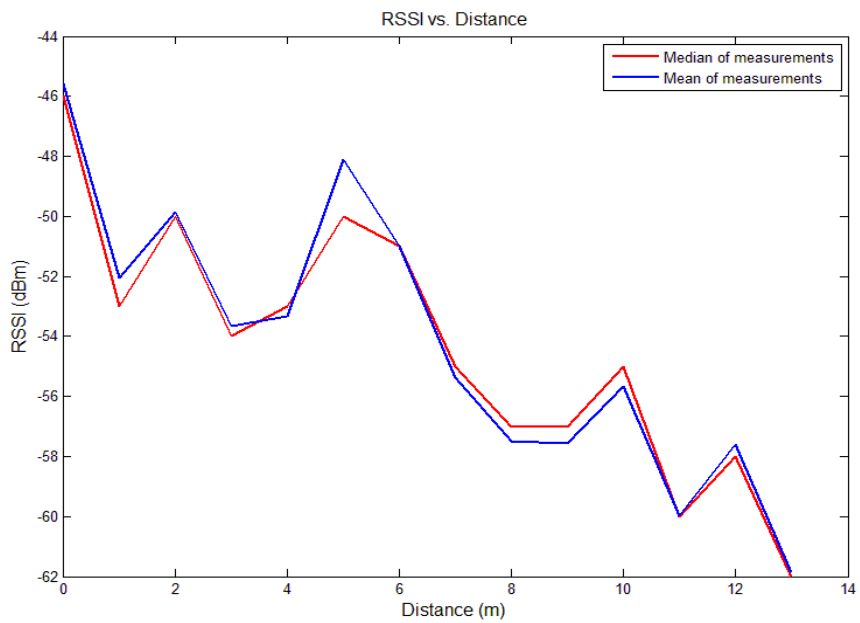


Figure 5.7: RSSI comportment at an indoor environment.

5.2 RF Propagation loss model

The RF propagation loss model is a mathematical expression representing the relationship between the RSSI and the distance between sender and receiver. The most widely used signal propagation model is the path loss model (PLM) (Chapter 3):

$$RSSI(d) = P_0 - 10n \log_{10} \left(\frac{d}{d_0} \right) \quad (6.1)$$

We apply the Least-Square Fitting method (LIF) in order to find the best-fitting curve through the RSSI values collected at both experiments performed outdoors and indoors.

5.2.1 Outdoor environment

For the experiment performed at the ‘Parc Mousouris’ we use the RSSI values collected up to 38 m distance. The coefficients for the best fit line $p(x) = ax + b$ are: $a = -28.5345$ and $b = -31.4316$. For (1) we deduce that:

$$p(x) = RSSI(d), \quad a = -10n, \quad x = \log_{10} \left(\frac{d}{d_0} \right) \quad \text{and} \quad b = P_0 \quad (6.2)$$

therefore $n = 2.853$ and $P_0 = -31.4316, d \in [2 \quad 38]$. The following figure depicts both the RSSI values and the best line fit in the least-square sense.

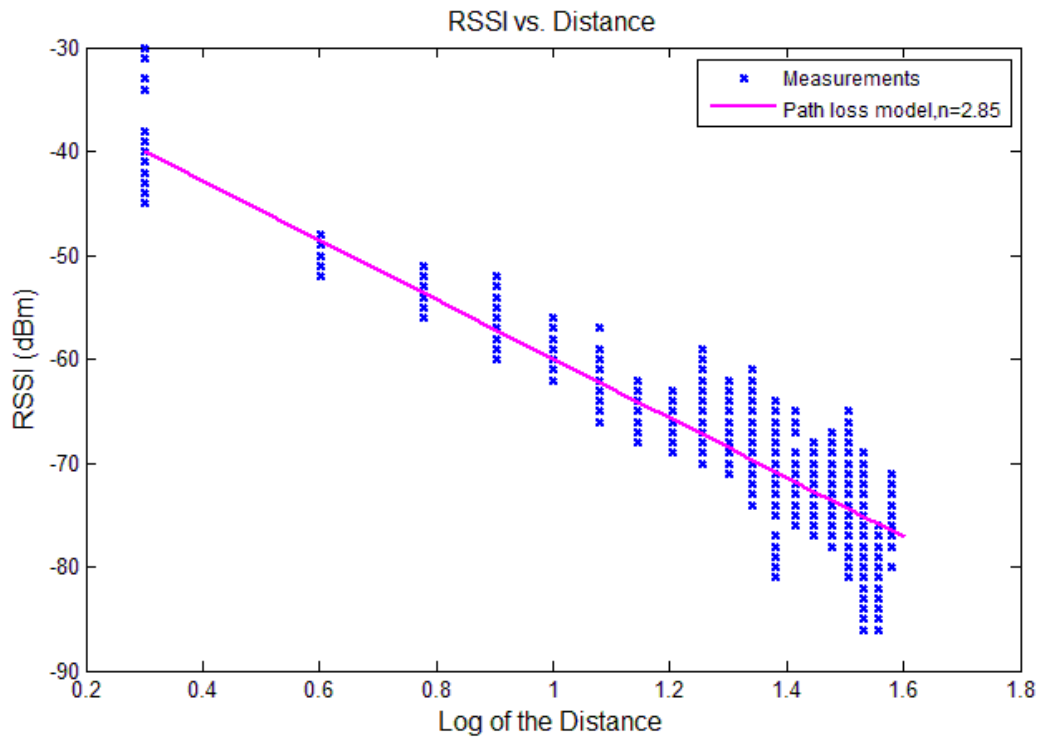


Figure 5.8: Outdoor propagation model for RSSI measurements.

5.2.3 Indoor environment

The coefficients for the best fit line are $a = -11.2657$ and $b = -45.4142$, from (6.2) we accumulate that $n = 1.127$ and $P_0 = -45.4142$. The following figure depicts both the RSSI values and the best line fit in the least-square sense.

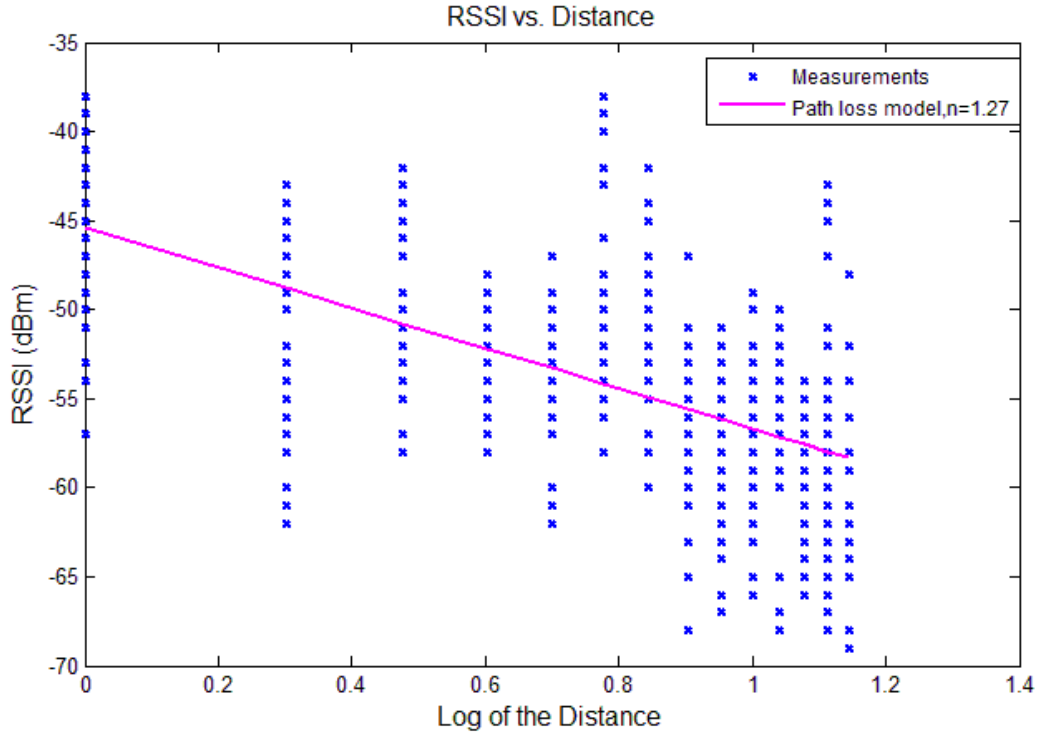


Figure 5.9: Indoor propagation model for RSSI measurements.

The radio propagation patterns in different environments exhibits the feature of non-isotropic path loss, i.e. radio signal attenuation varies along different directions [29]. We notice that every RSSI value that is equal or smaller than -64 dBm (Figure 5.4) for outdoor environments and -50 dBm (Figure 5.7) for indoor environments can actually correspond to any distance that is longer than 12 meters and 0.8 meters, respectively. Unfortunately, the maximum distance that this region of RSSI values can cover is very small.

In the Madwifi driver the reported RSSI for each packet is actually equivalent to the Signal-to-Noise Ratio (SNR) [30]. The RSSI reported by the MadWiFi HAL is a value in dBm that specifies the difference between the signal level and noise level for each packet. Hence the driver calculates a packet's absolute signal level by adding the RSSI to the absolute noise level. The driver does not get the noise reading for each and every packet but takes the measured noise level at each interrupt and assumes all packets serviced during the interrupt were received with this noise level. As a result, another approximation, in order to estimate the correlation between the distance and the RSSI, would be to retrieve the attenuation of the signal and not the SNR. However, the drawback of this approach is that it is not robust because it is dependent on the way of calculation of the noise level.

Based on the experiments described, we can conclude that if the RSSI value is high then we are confident that the receiver is close to the transmitter (Figure 5.4, Figure 5.7). However, if

the signal is low this might imply two things: either there is an obstacle between the receiver and the transmitter or their distance is high. Finally, this information could be used in order to adjust the weights w_{ij} (equation 3.15). The Energy function will give more importance to the high RSSI value while the transmitters with low RSSI values will have a small weight. This method could be improved more with the knowledge of the impact of the obstacles to signal strength.

Chapter 6

6. Conclusion

In this thesis, we discussed an improvement of Kamada-Kawai method for localization by adding supplementary constraints. We formulated the localization problem as a least square problem. The main objective is to find the coordinates of the unlocated node under the constraint that nonadjacent nodes should be placed far apart. We designed an energy function which is minimized satisfying this request using Newton-Raphson method. The proposed algorithm is ‘cooperative’ because the position of each node or sensor is decided based on some shared information related to its neighbors. Moreover, it is fully distributed, and does not rely on explicit communication apart from the one between immediate neighbors. The fully distributed nature of the algorithm is critical for a practical implementation in ad hoc networks.

We evaluated the performance of our algorithm via simulations in real-world conditions. We tested the accuracy of the Weighted Min Max localization method under a specific sensor deployment strategy in different environments. Particularly, the results were promising in the open-area environment. On the other hand, in the indoor environment we observed that the measurement errors increased due to reflection, diffraction and multipath of the signal.

Finally, we collected real RSSI measurements both in an indoor and an open-field environment. We observed that as the distance was increasing the signal-strength value was decreasing. Specifically, based on the RSSI value performance, we concluded that the maximum distance the RSSI values can cover is not as promising as it was expected. As a result, in a real outdoor environment, a high value of the signal indicates that the distance is small enough. However, when the value of RSSI is small the correlation between the RSSI and the distance is not obvious. This last observation forms a new challenge at the localization area.

7. References

- [1] Kamada T., Kawai S., 'An algorithm for drawing general undirected graphs' Information Processing Letters 31 (1989), pp.7-15
- [2] Theodore S. Rappaport, 'The Wireless Revolution', IEEE Communications Magazine, November 1991.
- [3] Biaz S., Ji Y., 'A survey and comparison on localization algorithms for wireless ad hoc networks', International Journal of Mobile Communications, v.3 n.4, p.374-410, May 2005.
- [4] Gansner E., Koren Y., North S., 'Graph Drawing by Stress Majorization', In Proceedings of the 12th Int. Symp. Graph Drawing, LNCS 3383, Springer Verlag, pp. 239–250, 2004
- [5] Hinckley K., Sinclair M., 'Touch-sensing input devices'. In Proceedings of the 1999 Conference on Human Factors in Computing Systems (CHI 1999). ACM, 1999.
- [6] Hightower J., Borriello G., 'Location Sensing Techniques', IEEE Computer Magazine, August 2001.
- [7] Niculescu, D., Nath, B. (2001) 'Ad hoc Positioning System (APS)', GLOBECOM 2001, San Antonio, November.
- [8] Enge P., Misra P., 'Special Issue on Global Positioning System', In Proceedings of the IEEE, January 1999.
- [9] Bahl P., Padmanabhan V., 'RADAR: An In-Building RF-based User Location and Tracking System', In Proceedings of IEEE Infocom 2000, Tel-Aviv, Israel March 2000.
- [10] Priyantha N., Chakraborty A., Balakrishnan H., 'The Cricket Location-Support System', In Proceedings of the 6th ACM MOBICOM, (Boston, MA), August 2000.
- [11] N. B. Priyantha, A. K. L. Miu, H. Balakrishnan, and S. Teller, 'The cricket compass for context-aware mobile applications', In Proceedings of the ACM/IEEE International Conference on Mobile Computing and Networking (MobiCom), (Rome, Italy), pp. 1–14, July 2001.
- [12] Want R., Hopper A., Falcao V., Gibbons J., 'The active badge location system', In Proceedings of the ACM Transactions on Information System, January 1992.

- [13] Federal Communications Commission. Fcc wireless 911 requirements fact sheet, January 2001. <http://www.fcc.gov/e911/>
- [14] Robert J. Orr and Gregory D. Abowd, ‘The smart floor: A mechanism for natural user identification and tracking’, In Proceedings of the 2000 Conference on Human Factors in Computing Systems (CHI 2000), The Hague, Netherlands, April 2000. ACM.
- [15] Harle R., Ward A., Hopper A., ‘Single reflection spatial voting’, In Proceedings of the First International Conference on Mobile Systems, Applications, and Services, (San Francisco), May 2003.
- [16] Hightower J., Borriello G., ‘A Survey and Taxonomy of Location Systems for Ubiquitous Computing’, Technical Report, University of Washington, Department of Computer Science and Engineering UW CSE 01-08-03, Seattle, WA, 2001.
- [17] Patwari N. and al., ‘Locating the nodes: cooperative localization in wireless sensor networks’, In Proceedings of the IEEE Signal Process. Mag., vol. 22, no. 4, pp. 54–69, 2005.
- [18] <http://www.navfltsm.addr.com/vor-nav.htm>
- [19] Ji, X., Zha, H., ‘Sensor positioning in wireless ad hoc sensor networks using multidimensional scaling’, In Proceedings of the IEEE INFOCOM, 2004
- [20] Premaratne K., Zhang J., Doguel M. ‘Location information-aided task-oriented self-organization of ad hoc sensor systems’, In Proceedings of the IEEE Sensors Journal, February, Vol. 4, No. 1, 2004
- [21] Savvides A., Park H., Srivastava M.B., ‘The n-hop multilateration primitive for node localization problems’, Journal of Mobile Networks and Applications (MONET), Vol. 8, pp.443–451, 2003
- [22] Niculescu D., Nath B., ‘DV Based Positioning in Ad Hoc Networks’, Kluwer Academic Publishers, 2003
- [23] Doherty, L. Kristofer, S., Pister, J., Ghaoui, L.E, ‘Convex position estimation in wireless sensor networks’, In Proceeding of IEEE Inforcom, Vol. 3, pp.1655–1663, 2001
- [24] Langendoen, K., Reijers, N. ‘Distributed location in wireless sensor networks: a quantitative comparison’, Computer Networks, Vol. 43, pp.499–518., 2003
- [25] Savarese, C., Langendoen, K., Rabaey, J. ‘Robust positioning algorithms for distributed ad hoc wireless sensor networks’, In Proceedings of the General Track: 2002 USENIX Annual Technical Conference, pp.317–327, 2002

- [26] Ramadurai, V., Sichitiu, M.L., ‘Localization in wireless sensor networks: a probabilistic approach’, In Proceeding of the 2003 International Conference on Wireless Networks (ICWN 2003), Las Vegas, NV, June, pp.275–281, 2003
- [27] Rappaport, T.S., Rappaport, T.: Wireless Communications: Principles and Practice, 2nd edn. Prentice-Hall, Englewood Cliffs (2001)
- [28] Lymberopoulos D., Lindsey Q., Savvides A. (2006) ‘An Empirical Characterization of Radio Signal Strength Variability in 3-D IEEE 802.15.4 Networks Using Monopole Antennas’, In Proceeding of the European Conference on Wireless Sensor Networks 2006 (EWSN 2006), Zurich, Swizerland, pp.326-341., 2006
- [29] Scott T, Wu K., Hoffman D. (2006) ‘Radio Propagation Patterns in Wireless Sensor Networks: New Experimental Resutls’, In Proceeding of the 2006 international conference on Communications and mobile computing (IWNC 2006),2006
- [30] <http://madwifi-project.org/wiki/>
- [31] <http://www.mathworks.com/>